People`s Democratic Republic of Algeria

Ministry of Higher Education and Scientific Research

University of Echahid Hamma Lakhdar - El Oued

Faculty of Technology

Department of Mechanical Engineering

Dissertation

ACADEMIC MASTER

Domain: Science and Technology

Division: Mechanics

Specialty: Electromechanical

Presented by:

Belkacmi Oualid

Ghouli Yahia

Ghemam Djeridi Mohammad

Entitled:

Optimization of Photovoltaic System Performance Using Advanced MPPT Techniques (P&O and INC,ANN).

Dissertation Submitted in Partial Fulfillment of the Requirements for the Master

Electromechanical

Degree in:18

Publicly defended in: 28/05 /2025

Board of Examiners:

Dr. BEGGAT FATEH	**Chairman**
Dr. MILOUDI KHALED	**Supervisor**
Dr. BEBBOUKHA ALI	**Co-supervisor**
Dr. LARGOT SOULEF	**Examiner**

Academic Year: 2024/2025

Dedication

First and foremost, I thank Allah for granting me the strength and patience to complete this work despite the challenges I faced.

I dedicate this work to:

My dear parents, and my beloved brothers and sisters.

To all my family members and friends who supported me.

To all those who love me and whom I love.

To my friends throughout my academic journey.

I would like to especially dedicate this work to Dr. Khaled Miloudi, my esteemed supervisor, who greatly contributed to my guidance. I also dedicate this work to Dr. Ali Bebboukha for his continuous assistance and support.

Acknowledgments

In the name of Allah, the Most Gracious, the Most Merciful

I begin by thanking Allah for granting me the success to complete this academic work, and I am grateful for His countless blessings.

I would like to express my sincere thanks and appreciation to Dr. Khaled Miloudi**,** my esteemed supervisor, for his valuable guidance and continuous support throughout my studies. I also thank Dr. Ali Bebboukha for his valuable assistance and guidance, which helped me in completing this work.

I would also like to express my gratitude to the honorable committee for their valuable time and attention in evaluating this work, as well as to the respected professors who contributed their advice and remarks, which enriched the development of this research

Abstract

Solar radiation serves as the primary energy source for photovoltaic (PV) systems, which convert sunlight directly into electricity through the photovoltaic effect. This study explores the fundamental concepts of PV systems and solar energy generation, considering variations due to location and seasonality. DC-DC converters play a vital role by efficiently converting voltage levels for stable power delivery.

To maximize PV system efficiency, Maximum Power Point Tracking (MPPT) algorithms continuously optimize the operating point to extract maximum power from solar panels under varying conditions. Three widely used MPPT algorithms – Perturb and Observe (P&O), Incremental Conductance (INC), and Artificial Neural Network (ANN) – are evaluated and compared.

The P&O algorithm relies on perturbations and observations, INC uses incremental conductance, while ANN leverages artificial intelligence for precise maximum power point tracking. This comprehensive analysis highlights the strengths, weaknesses, and suitability of each algorithm, providing insights to improve the overall performance and energy yield of PV systems.

Keywords:

Photovoltaic systems (PV), Maximum Power Point Tracking (MPPT), Solar energy Artificial Neural Networks (ANN), Perturb and Observe (P&O), Incremental Conductance (INC).

الملخص:

تُعتبر الإشعاع الشمسي المصدر الرئيسي للطاقة بالنسبة لأنظمة الطاقة الكهروضوئية(PV) ، والتي تحول ضوء الشمس مباشرةً إلى كهرباء من خلال التأثير الكهروضوئي. تستكشف هذه الدراسة المفاهيم الأساسية لأنظمة الطاقة الكهروضوئية وتوليد الطاقة الشمسية، مع الأخذ بعين الاعتبار التغيرات الناجمة عن الموقع والموسمية. تلعب محولات التيار المستمر (DC-DC) دوراً حيوياً من خلال تحويل مستويات الجهد بكفاءة لتوفير إمداد طاقة مستقر.

لتحقيق أقصى كفاءة لأنظمة الطاقة الكهروضوئية، تعمل خوارزميات تتبع نقطة الطاقة القصوى (MPPT)على تحسين نقطة التشغيل باستمرار لاستخراج أقصى قدر من الطاقة من الألواح الشمسية في ظل ظروف متغيرة.

تتم تقييم ومقارنة ثلاث خوارزميات MPPT واسعة الاستخدام - خوارزمية الاضطراب والمراقبة (P&O)، وخوارزمية التوصيل التفاضلي(INC) ، وشبكة الخوارزميات العصبية الإصطناعية(ANN).

تعتمد خوارزميةP&Oعلى الاضطرابات والملاحظات، بينما تستخدم خوارزمية INC التوصيل التفاضلي، في حين تستفيد خوارزمية ANN من الذكاء الاصطناعي لتتبع نقطة الطاقة القصوى بدقة. تُلقي هذه التحليلات الشاملة الضوء على نقاط القوة والضعف وملاءمة كل خوارزمية، وتوفر رؤى لتحسين الأداء الإجمالي وعائد الطاقة لأنظمة الطاقة الكهروضوئية.

الكلمات المفتاحية:

أنظمة الخلايا الضوئية(PV)، تتبع أقصى نقطة للقدرة(MPPT) ، الطاقة الشمسية، الشبكات العصبية الاصطناعية (ANN)، خوارزمية الاضطراب والمراقبة (P&O)، خوارزمية التوصيل التفاضلي(INC)

Contents

Chapter II: DC-DC Converter

Chapter III: Maximum Power Point Tracking

Chapter IV: Simulation Results

List of Figures

List of Tables

List of Acronyms and Abbreviations

List of Abbreviations	
PV	Photovoltaic
MPP	Maximum power point
MPPT	Maximum power point tracking
P&O	Perturb and observe
INC	Incremental Conductance
ANN	Artificial neural network
DC-DC	Continuous-continuous converter
KVL	Kirchhoff's Voltage Law
PWM	Pulse Width Modulation
LED	Light Emitting Diode
MOSFET	Metal Oxide Semiconductor Field Effect Transistor

List of Acronyms	
D	The duty cycle
T	The total time period (S)
CH	The chopper
$f_{\text{switching}}$	The switching frequency (kHz)
G	The conductance value(1000 W/m^2)
R_{opt}	The optimal value of the load resistance(Ω)
$\mathbf{R_c}$	The load resistance(Ω)
$\mathbf{V_{oc}}$	Open circuit voltage (V)
$\mathbf{I_{oc}}$	Open circuit current(A)
Rs	Series resistance(Ω)
Rsh	Shunt resistance (Ω)
L	Inductance (mH)

C	Capacitance (µF)
I_{sc}	The short circuit current (A)
Pmax	The value of the maximum real power (W)
η	The energy efficiency of the solar cell (%)
$P\gamma$	The incident light power on the surface of the cell
V_L	The voltage across the inductor (V)
W_{on}	The energy input provided by the source to the inductor when CH is on
W_{off}	The energy that the inductor releases to the load when CH is off

General Introduction

General Introduction

The world population is increasing rapidly, and energy consumption is rising. Consequently, greater electricity production is necessary to meet human needs, leading to an increase in the amount of resources required to produce it. However, the resources that have been primarily used so far, fossil fuels, are finite resources. Therefore, it is necessary to explore energy sources that are not depleted.

Solar energy certainly represents the most elegant renewable energy source. In addition to being silent, it integrates perfectly into buildings (facades, roofs, etc.), and because it does not include moving mechanical parts, it does not require special maintenance and remains reliable for a long time. This is why it has become a reference in space applications and in isolated sites. It is becoming a reliable option for small and medium energy consumption applications, especially since solar panels have become cheaper for better efficiency[1].

In this work, we study the improvement of efficiency and performance of photovoltaic solar energy production systems using a maximum power point tracking (MPPT) controller with changes in ambient weather conditions such as solar radiation and temperature. In this context, the work aims to simulate a photovoltaic energy production system consisting of a solar panel, and a DC/DC boost converter.

Chapter I

Solar Radiationand

Photovoltaic Energy

I.1. Introduction :

Solar radiation is the energy produced by the sun as a result of ongoing nuclear reactions in its core, where hydrogen atoms fuse to form helium in a process known as nuclear fusion. During this process, the Sun releases huge amounts of energy that spread through space in the form of electromagnetic waves.

Part of this energy reaches the Earth, being the primary source of life and forming the basis for many natural processes, such as the water cycle and photosynthesis in plants.

As for photovoltaic energy, it is a technology that converts solar radiation directly into electrical energy using solar cells.

This technology is based on the photoelectric effect discovered by the scientist Albert Einstein, where photons (light particles) have enough energy to release electrons inside semiconductor materials, which leads to the generation of an electric current.

I.2. Solar Radiation:

is a group of visible electromagnetic rays that a person can see. These rays pass through the atmosphere, and the atmosphere absorbs some of them and leaves some of them for us to reach the Earth [1].

Solar radiation as it passes through the atmosphere is subject to absorption and scattering. About 30 percent of solar radiation is reflected back into space. About 20 percent is absorbed by clouds and particles in the air. The amount of solar radiation that ultimately reaches the Earth's surface depends on the concentration of atmospheric particles, gaseous pollutants, and water (vapor, liquid, or solid). [1] [2]

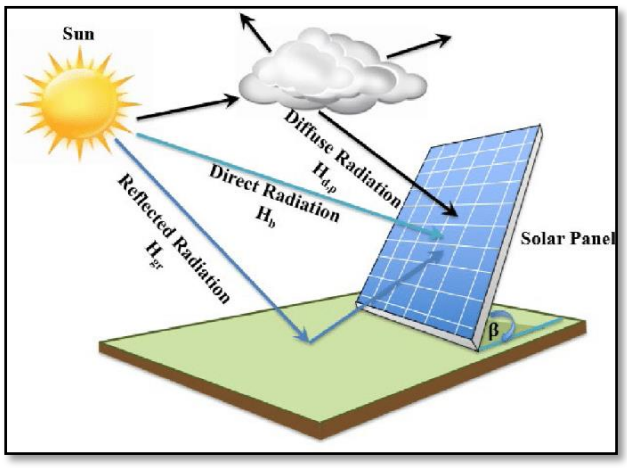

Figure (I.1): Representation of Solar Radiation.

I.3. Radiation Spectrum:

The solar constant represents all the energy in the solar spectrum. By observing the radiation, it was found that it consists of a group of electromagnetic waves whose length ranges from 0.11 microns to 4 microns. In fact, solar radiation contains longer. positive wavelengths, but the amount of energy in it is very small and does not exceed 1% of the total solar spectrum energy [3].

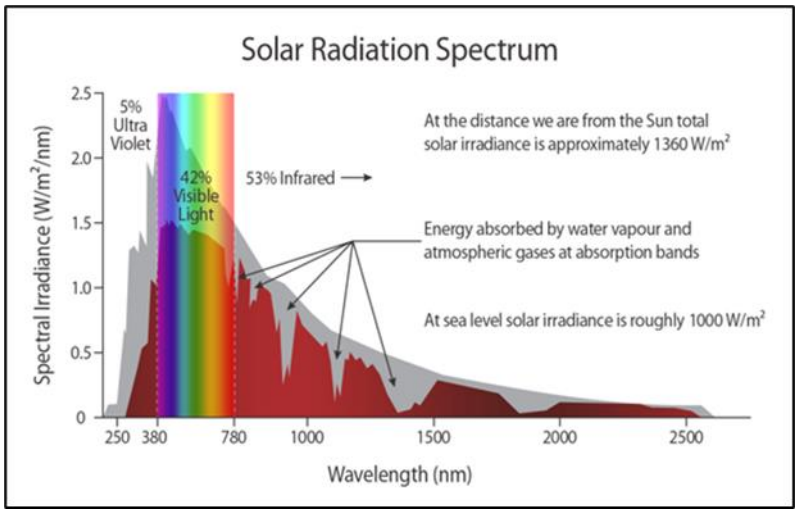

Figure (I.2): Representation of Solar Radiation Spectrum.

I.4. Conversion of Solar Radiation by PV Effect:

Solar radiation consists of photons ranging in wavelength from ultraviolet (UV) radiation (0.2 micrometers) to far infrared 2.5 micrometers. The concept of AM (Air-Mass) is used to characterize the solar spectrum in terms of the energy emitted.

The total energy transferred by solar radiation at a distance between the Sun and the Earth is in the range of 1350 W/per square meter (AM0) in space outside the Earth's atmosphere Figure.(4.1) When solar radiation passes through the atmosphere, it undergoes attenuation and modification of its spectrum as a result of absorption and diffusion phenomena in gases, water Thus, the ozone layer absorbs part of the light spectrum from the sun, especially part of the ultraviolet rays that pose a risk to health.[4]

The direct solar radiation received at ground level (at 90°F) reaches up to 1000 W/meter due to absorption in the atmosphere. (AM1) This value changes depending on the tilt of the light rays relative to the Earth. The smaller the θ angle of penetration, the thicker the atmosphere that must absorb the rays.

This results in energy loss as a result. For example, the direct energy carried by solar radiation reaching the Earth at an angle of 48° is approximately 833 W/m2 (AM1.5).[5]

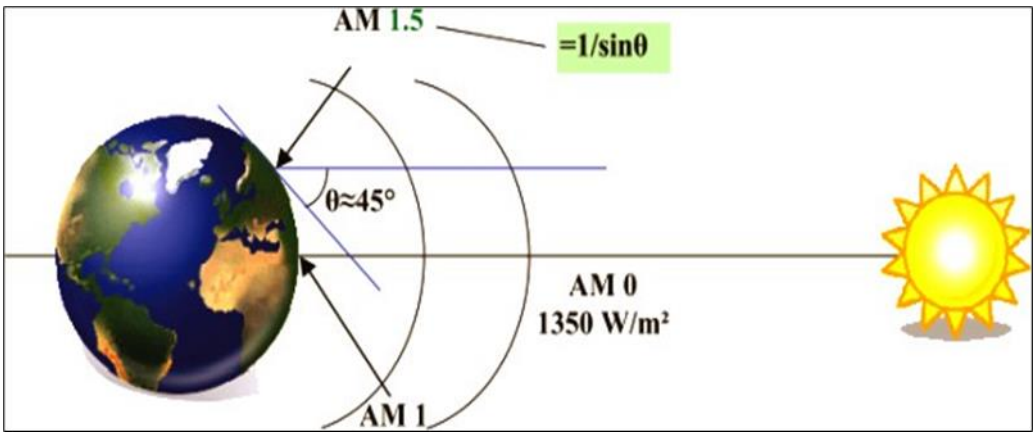

Figure (I.3): Standard for measuring the spectrum of light energy emitted by the Sun.

I.5. Photovoltaic Generator:

A photovoltaic cell is based on a physical phenomenon called the photoelectric effect, which consists of the creation of an electromotive force at the surface of the cell where it is exposed to light. The voltage generated can vary between 0.3 V and 0.7 V according to the materials used and their arrangement as well as the temperature of the cell and the aging of the cell. Figure (1.5) shows a schematic diagram of a photovoltaic cell. [6]

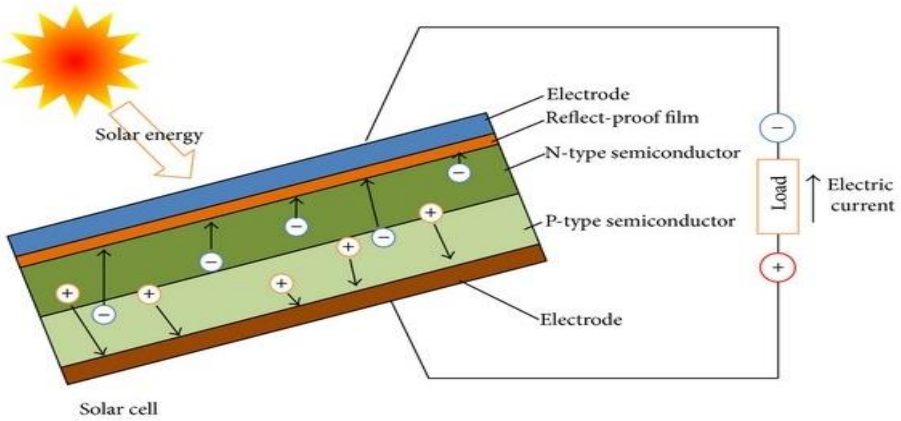

Figure (I.4): Schematic diagram of a photovoltaic cell.

When sunlight falls on a solar cell, it passes through the cell's surface, where part of it is absorbed by the first layer of the cell, which is the layer containing phosphorus. As for the majority of the light falling on this cell, it is absorbed by the part that contains two layers of crystalline silicon, where this process creates free-moving electrons that can flow through the electrical conductor at the cell's terminals, and this movement increases as the intensity of the light falling on the cell increases.

We can connect an electrical load on the terminals of this cell and take advantage of the movement of electrons resulting from the fall of sunlight, and Figure (2.2) shows how the photovoltaic cell works. [7]

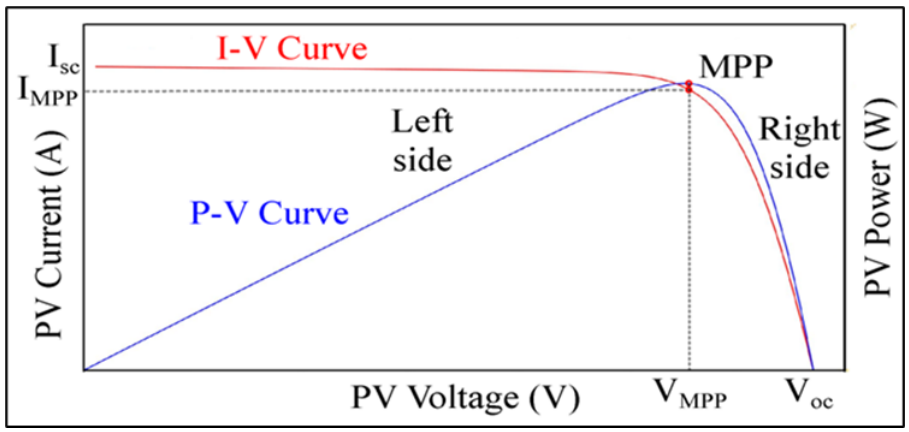

Figure (I.5): Typical Characteristics of a PV Generator.

I.6. Photovoltaic Cell:

The photovoltaic system consists of a group of cells which are the basic element in this system, where one can reach the appropriate power based on a certain composition.

Photovoltaic cells are photoelectronic components that convert sunlight directly into electricity The current obtained is direct current (CC) [8].

They are manufactured using semiconductor materials that have properties intermediate between conductors and insulators.

This semiconductor is located between two metal electrodes and the whole is protected by glass [9].

The basic material in most cases is silicon (Si), cadmium sulfide (CdS) or cadmium telluride (CdTe).

Depending on the manufacturing process, more or less efficient solar cells will be obtained [10].

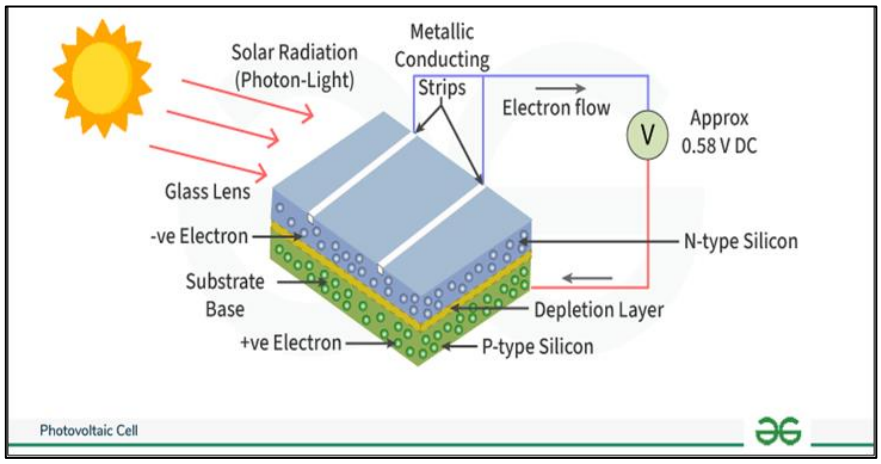

Figure (I.6): The solar cell and its mechanism of converting solar energy into electrical energy.

1.6.1. Modelling of a PV Cell:

The photovoltaic cell is the basic unit of a photovoltaic module and is the element responsible for transforming the sun's rays or photons directly into electrical energy.

The equivalent circuit of a photovoltaic cell is shown in Figure 1.6.1[11].

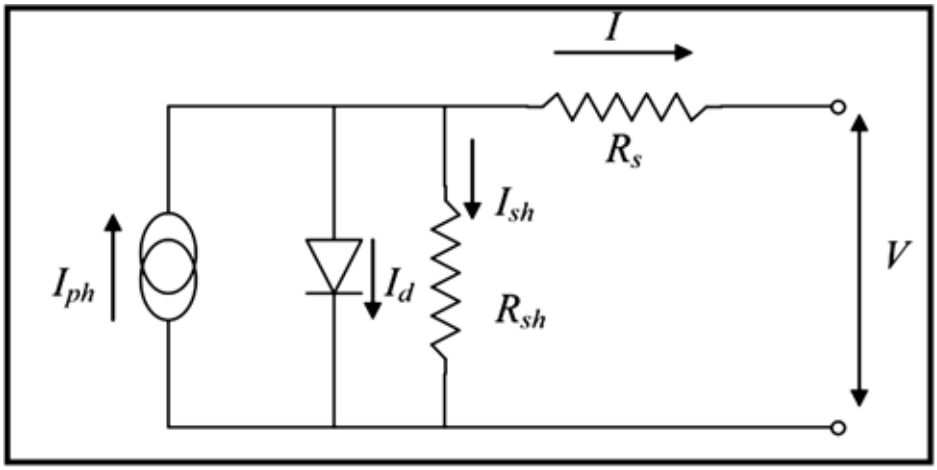

Figure (I.7): Equivalent circuit of a photovoltaic cell.

1.6.2. Types of Photovoltaic Cells :

Photovoltaic solar panels are made up of photovoltaic cells and vary according to type:

1.6.2.1. Monocrystalline Cells:

Most photovoltaic cells manufactured until recently were made of pure, continuous, single-crystal silicon without impurities. Single-crystal silicon is usually made of small grains of crystal slowly drawn from a melted mass of polycrystalline silicon in an advanced and expensive way. Most single-crystal silicon cells available in the market have an efficiency of about 16%. Despite the high efficiency advantage of the single-crystal solar cell, its price is very high because it is made of single-crystal silicon and of high purity, and because the manufacturing method is expensive and requires skilled workers. Some cells are currently manufactured from less pure silicon. These cells are cheaper and produced at a lower cost using different, low-cost processes, but they are less efficient and have a shorter lifespan [12].

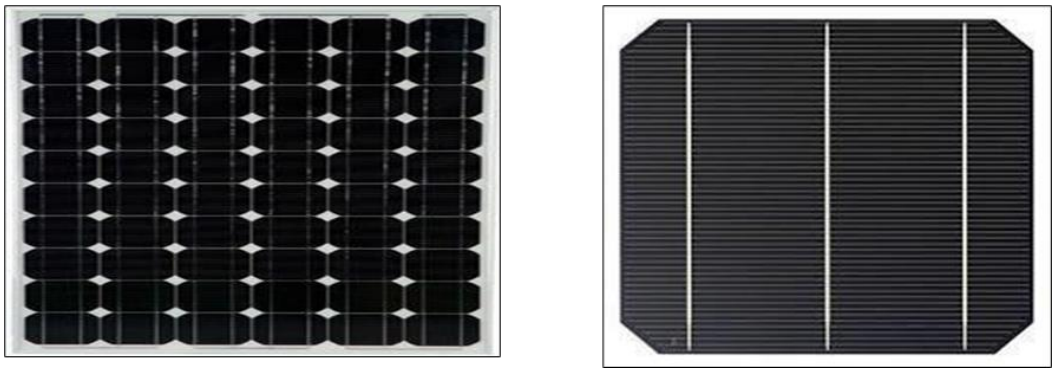

Figure (I.8): Monocrystalline silicon cell and solar panel made of monocrystalline cells.

.1.6.22.Polycrystalline Cells:

It consists of silicon chips scraped from cylindrical silicon crystals, then chemically treated in ovens to increase their electrical properties. After coating, the surfaces of the cells are covered with anti-reflection so that the cells absor b sunlight with high efficiency. The efficiency of this type is from 9 to 13%[13].

figure (I.9): Polycrystalline silicon cell and solar panel made of polycrystalline cells.

.1.6.23. Hydrogenated Amorphous Cells:

Amorphous silicon is obtained from silicon gas. This gas is vaporized onto a support, either glass, flexible plastic, or metal, using a vacuum deposition process. These PV cells are dark gray.

Figure (I.10): Hydrogenated Amorphous Cells.

I.7. The Impact of Temperature on Solar Panel:

Temperature has a significant impact on the performance of solar panels. Here's how:

The rise in weather temperature leads to an increase in the temperature of the solar cell, which in turn leads to a decrease in the produced current and open circuit voltage of the photovoltaic cell, and also results in a slight increase in the short circuit current of the solar cell, as shown in Figure [14].

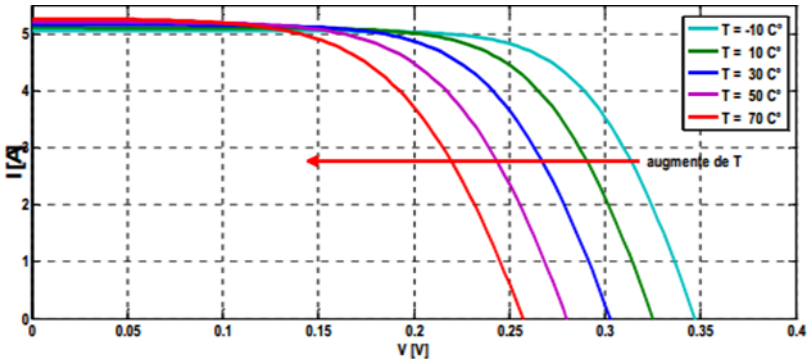

Figure (I.11): Current versus voltage curve with temperature change.

I.8. Uses of solar radiation and photovoltaic energy

Solar radiation is the primary source of renewable energy, and is used in many ways to convert it into electricity or heat. Here are some of the most important uses of solar radiation and photovoltaic energy with illustrative images.

1.8.1. Electricity generation using photovoltaic panels

It depends on converting sunlight directly into electricity using solar cells made of silicon.

It is used in homes, commercial buildings, and solar farms [15].

Figure (I.12): Photo of a solar panel system installed on the roof of a house.

1.8.2. Operating devices and equipment in remote areas

Solar energy is used to power communications, lighting, and sensors in remote areas.

Useful in remote villages, roadside light poles, and scientific stations[16].

Figure (I.13): Solar-powered light pole.

1.8.3. Solar-powered pumping and irrigation systems

Solar-powered water pumps are used to irrigate agricultural fields, especially in remote areas.

They reduce the need for fossil fuels and efficiently provide irrigation water [17].

Figure (I.14): Solar-Powered Water Pumping System for Agricultural Irrigation.

1.9.Advantages and Disadvantages of PV Energy:

1.9.1. Advantages

- First, it is characterized by high reliability, as the system has no moving parts, making it particularly suitable for isolated areas. This is why it is used on spacecraft.
- Second, the modularity of PV panels allows for simple installation and adaptability to a variety of power needs. Systems can be designed to meet power requirements ranging from milliwatts to megawatts.
- Third, the cost of operation is very low due to low maintenance, and it does not require fuel, transportation, or highly specialized personnel.
- Finally, PV technology has environmental advantages, as the final product is non-polluting, silent, and does not cause any disturbance to the environment, except for taking up space in large-scale installations [18].

1.9.2. Disadvantages:

- The manufacturing of solar photovoltaic panels relies on advanced technology that requires a lot of research and development, necessitating heavy investments. This is reflected in the installation price, which is still high today.
- The efficiency of PV panels is still low, around 20% at best. Therefore, PV is more suitable for projects with low needs, such as individual homes.
- In the case of an autonomous PV system that does not sell surplus electricity to the grid, batteries must be used, the cost of which remains very high.
- The level of electricity production is unstable and unpredictable, as it depends on the level of solar radiation. In addition, no electricity is produced in the evening or during the night.
- The lifespan of a PV system is not permanent, ranging from 20 to 30 years. Moreover, the performance of photovoltaic cells degrades over time, with an estimated efficiency loss of 1% per year in general. [19].

1.10. Conclusion:

This chapter covered the basics of solar radiation and photovoltaic energy conversion, explaining how electricity is generated by solar cells. It also discussed the modeling and characteristics of photovoltaic generators and the factors affecting their efficiency, such as temperature and load resistance. The types of photovoltaic cells and their components are discussed, highlighting the main advantages and disadvantages of this technology.

Chapter II

DC-DC Converter

II.1. Introduction :

DC-DC converters are essential electronic circuits that play a critical role in modern power management systems. Their primary function is to convert the voltage of a direct current (DC) source from one level to another, ensuring stable and efficient power delivery to various electronic devices and systems. In applications where input voltage levels can fluctuate due to factors such as battery discharging over time or changes in load conditions, DC-DC converters maintain a constant output voltage, providing reliable power to the system's components. One significant advantage of DC-DC converters is their superior power conversion efficiency. By using switching techniques, they can minimize power losses associated with resistive elements, such as transformers or linear regulators, which typically generate heat and waste energy. This results in better overall efficiency and prolonged battery life in portable devices. Moreover, DC-DC converters offer the flexibility to step up or down voltage levels, allowing for efficient power distribution management in electronic systems. They can also provide galvanic isolation, separating the input and output grounds to reduce the risk of ground loops and safeguard sensitive components from voltage spikes and noise.

II.2. DC-DC Converters:

"DC-DC converters are static power electronic devices that operate using a DC voltage source to generate a controllable DC output voltage across a load. These converters can be designed using thyristors for high-power applications, reaching several hundred megawatts, with a chopping frequency in the range of a few kilohertz. Alternatively, for lower power levels—typically up to 100 kW—transistors are employed, enabling higher chopping frequencies of up to 100 kHz. The following figure presents the symbolic representation of a DC-DC converter.".

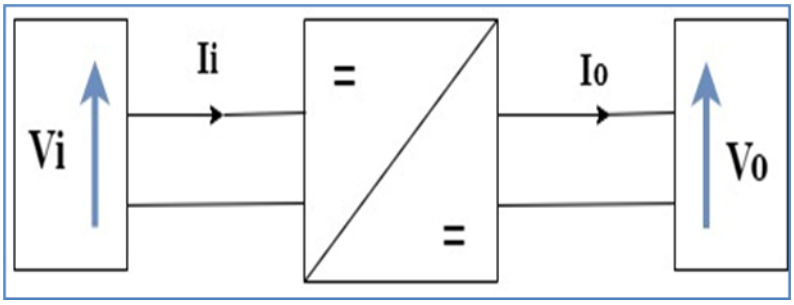

Figure (II.1): DC-DC Converters

II.3. Applications of DC-DC Converter:

"For several years, switch-mode power converters have been extensively utilized in modern electronics across various sectors, including industrial, commercial, utility, and consumer markets. In low-power DC-DC conversion applications, power conversion is predominantly achieved through three fundamental types of converters: buck, boost, and buck-boost. However, specialized applications may require advanced configurations or modified versions of these conventional topologies to meet specific operational demands.

There are several DC-DC converter types in the literature, but there is no one solution that caters to all the applications. Conversion techniques, in general, have found a wide array of applications in industry, research and development, and daily life[20]**.**

DC-DC converters form a key aspect of study in the field of power electronics and energy drives as they are widely incorporated in several industrial applications. Some of the applications are illustrated in Figure (II.2). High voltage gain converters are employed in multiple sophisticated applications, including radar systems, DC distribution systems, data centers, and harnessing renewable energy[21]**.**

"This is particularly essential in renewable energy applications, where high-voltage-gain DC-DC converters enable voltage amplification, making it suitable for integration with the distribution system. In general, DC distribution provides numerous advantages, including a reduced number of conversion stages, cost-effectiveness, and improved power quality, thereby making it a preferred choice for a wide range of applications.

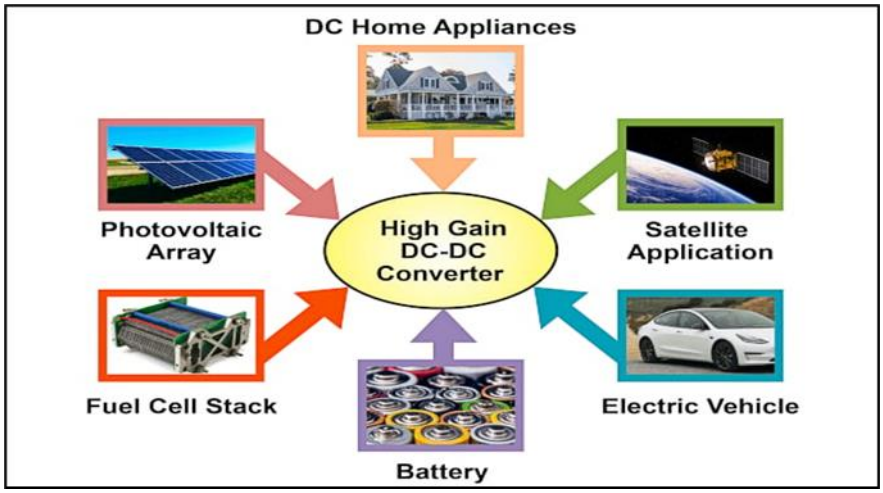

Figure (II.2): Applications of DC/DC Converters.

Here are some of DC-DC converter applications:

- **Renewable energy applications:** The DC-DC converter types employed for renewable energy applications need to draw continuous and smooth input current so ripple reduction can be achieved. It should also be able to integrate with different types of power sources. Non-isolated interleaved high voltage gain types are typically employed for interfacing renewables and micro grids[22]**.**
- **Medical devices**"Isolated DC-DC converters play a vital role in applications where safety is a primary concern, as they ensure electrical isolation between the output and potentially hazardous input voltages. This isolation is essential for preventing electrical hazards and ensuring system reliability. However, non-isolated converters can be utilized in applications such as the power supply for X-ray systems, where isolation is not a strict requirement.
- **Vehicles:** In the case of vehicles, the main DC-DC converter changes power from the onboard high voltage battery into lower DC voltages used to power lights, wipers, and window controls [23]**.** "This applies to both electric vehicles and hybrid electric vehicles. Isolation is essential in scenarios where the separation of control systems from high-voltage domains is required to ensure safety and reliability. Buck-boost converters are employed for voltage step-up or step-down applications, while charge-pump converters are utilized for voltage inversion.

- **Smart lighting:** "Various lighting applications necessitate LED backlight driver solutions characterized by high efficiency, precise direct current control, voltage protection, PWM-based regulation, and a straightforward design. Effective DC-DC converter types used as drivers include linear regulators, charge pumps, and other conventional switching converters

II.4. Types of DC-DC converters:

There are three types of DC-DC converters, namely: Buck, Boost, and Buck-Boost.

II.4.1. Buck Converter:

"A buck converter is a type of DC-DC converter specifically designed to perform step-down conversion of the applied DC input voltage. In buck converters, a fixed DC input is transformed into a lower-magnitude DC output. This implies that the converter is engineered to generate a DC output voltage that is lower than the applied input voltage. It is also referred to as a Step-Down DC-DC Converter, Step-Down Chopper, or Buck Regulator.

Operating Principle of Buck Converter

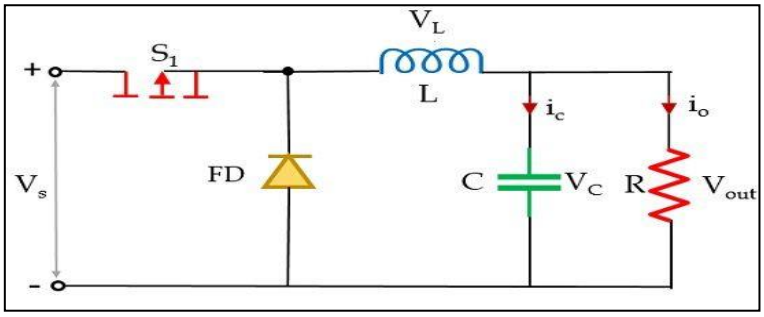

Figure (II.3): The Circuit Representation of Buck Converter

"In the figure above, it is evident that, in addition to the power electronics solid-state device functioning as a switch within the circuit, a freewheeling diode serves as a secondary switch. The combination of these two switching elements is integrated with a low-pass LC filter to minimize current and voltage ripples, thereby facilitating the generation of a regulated DC output. A pure resistive load is connected across this arrangement, serving as the circuit's load.

"The circuit operates in two distinct modes. The first mode occurs when the power MOSFET, denoted as switch S1, is in a closed state. In this operational mode, the closure of switch S1 permits the flow of current through the circuit."

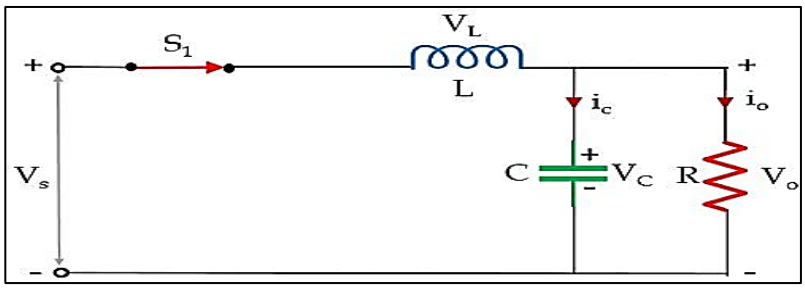

Figure (II.4): Buck Converter When S_1 is Closed

"When a fixed DC voltage is initially applied to the input terminals of the circuit, and switch S1 is in the closed state, current flows through the circuit as depicted above. As a result of this current flow, the inductor in the circuit stores energy in the form of a magnetic field. Additionally, the presence of a capacitor in the circuit allows current to pass through it, leading to charge accumulation. Consequently, the voltage across the capacitor appears across the load.

"However, in accordance with Lenz's law, the energy stored in the inductor opposes the change that induced it. As a result, an induced current is generated, leading to a reversal of the polarity across the inductor.

Here the total time period is a combination of T_{on} and T_{off} time.

$$T = T_{on} + T_{off} \quad \text{(II. 1)}$$

The duty cycle is written as:

$$D = \frac{T_{on}}{T} \quad \text{(II. 2)}$$

On applying KVL, in the above-given circuit

$$V_s = V_L + V_{\text{out}} \quad \text{(II. 3)}$$

$$V_L = V_s - V_{\text{out}} \quad \text{(II. 4)}$$

Also,

$$V_L = L\frac{di_L}{dt} = V_s - V_{\text{out}} \qquad \text{(II. 5)}$$

$$\frac{di_L}{dt} = \frac{V_s - V_{out}}{L} \qquad \text{(II. 6)}$$

When S1 is in closed condition then T_{on} = DT thus Δt = DT. Therefore, we can write

$$\frac{\Delta i_L}{\Delta t} = \frac{V_s - V_{\text{out}}}{L} \qquad \text{(II. 7)}$$

$$\frac{\Delta i_L}{DT} = \frac{V_s - V_{\text{out}}}{L} \qquad \text{(II. 8)}$$

Hence,

$$\Delta i_t = \left(\frac{V_s - V_{\text{out}}}{L}\right) DT \qquad \text{(II. 9)}$$

The above equation represents the change in current through the circuit when switch S1 is closed.

The second mode of operation occurs when switch S2 is closed, and switch S1 is opened. A question may arise regarding how switch S2 closes automatically. As previously discussed, the inductor in the circuit stores energy. Therefore, when S1 opens, the inductor begins to function as a source. In this mode, the inductor releases the energy stored during the previous phase of operation. Given that the polarity of the inductor reverses, the freewheeling diode, which was previously in a reverse-biased state due to the applied DC input, becomes forward-biased. Consequently, the current flows in the manner illustrated below:

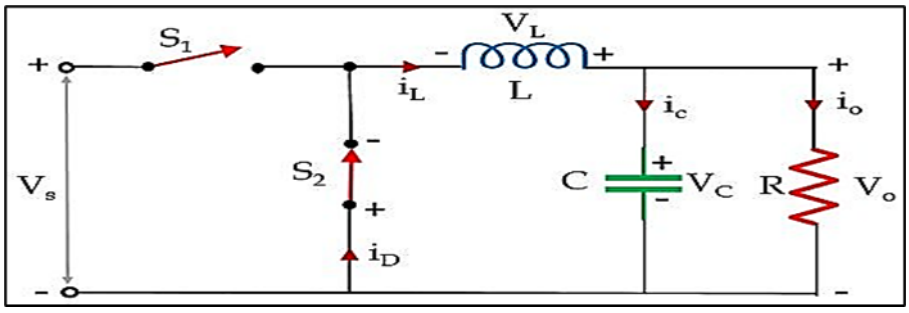

Figure (II.5): Buck Converter When S_2 is Closed

This current flow will persist until the energy stored within the inductor is entirely dissipated. Once the inductor is fully discharged, the diode transitions to a reverse-

biased state, resulting in the opening of switch S2. Subsequently, switch S1 closes instantly, and the cycle repeats.

Now, let us apply KVL, in the above circuit

$$0 = V_L + V_{\text{out}} \tag{II.10}$$

$$V_L = L\frac{di_L}{dt} = -V_{\text{out}} \tag{II.11}$$

Since, we know,

$$\mathrm{T} = \mathrm{T_{on}} + \mathrm{T_{off}} \tag{II.12}$$

$$\mathrm{T} = \mathrm{DT} + \mathrm{T_{off}} \tag{II.13}$$

$$\mathrm{T_{off}} = \mathrm{T} - \mathrm{DT} \tag{II.14}$$

$$\mathrm{T_{off}} = (1 - \mathrm{D})\mathrm{T} \tag{II.15}$$

$$V_L = L\frac{\Delta i_L}{\Delta t} = -V_{\text{out}} \tag{II.16}$$

$$\mathrm{T_{off}} = \Delta\mathrm{t} = (1 - \mathrm{D})\mathrm{T} \tag{II.17}$$

$$L\frac{\Delta i_L}{(1-D)T} = -V_{\text{out}} \tag{II.18}$$

So,

$$\Delta i_L = -\frac{V_{\text{out}}}{L}(1-D)T \tag{II.19}$$

This equation represents the rate of change in current through the inductor when the switch S1 is open.

As we know that the net change of current through the inductor in one complete cycle is zero. Thus,

$$\Delta i_{L_{(s1-closed)}} + \Delta i_{L(S1-\text{ open })} = 0 \qquad (\text{II. } 20)$$

$$\frac{V_s - V_{\text{out}}}{L} DT + \left\{ -\frac{V_{\text{out}}}{L} (1 - D)T \right\} = 0 \qquad (\text{II. } 21)$$

On simplifying,

$$\frac{V_s DT}{L} - \frac{V_{\text{out}}\, DT}{L} - \frac{V_{\text{out}}\, T}{L} + \frac{V_{\text{out}}\, DT}{L} = 0 \qquad (\text{II. } 22)$$

$$\left(\frac{V_s DT}{L}\right) = \frac{V_{\text{out}}\, T}{L} \qquad (\text{II. } 23)$$

$$V_{\text{out}} = DV_s \qquad (\text{II. } 24)$$

The figure given below represents the waveform representation of Buck Converter:

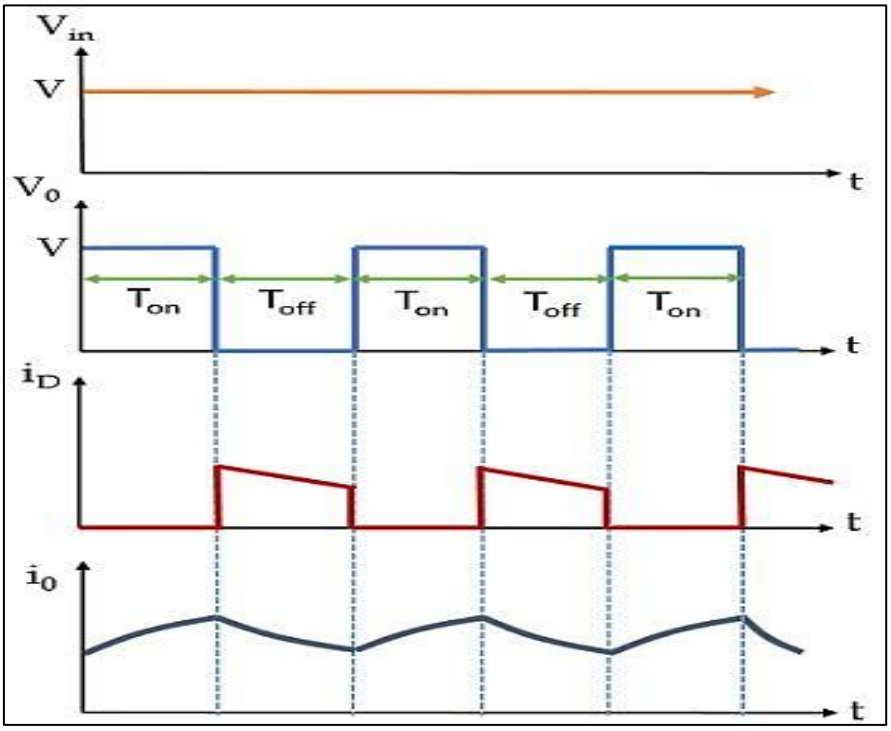

Figure (II.6): Waveform Representation

Hence, we can say, buck converters are used to provide a lower value of dc signal from a fixed dc input.

II.4.2. Boost Converter:

Boost converters, also referred to as step-up DC-DC converters, are a type of chopper circuit designed to generate an output voltage greater than the supplied input

voltage. In boost converters, DC-to-DC conversion occurs in such a way that the circuit delivers an output voltage of higher magnitude than the input voltage. The term 'boost' is used to signify that the output voltage is elevated relative to the input voltage

Operating Principle of Boost Converter

The figure given below is the circuit representation of the boost converter:

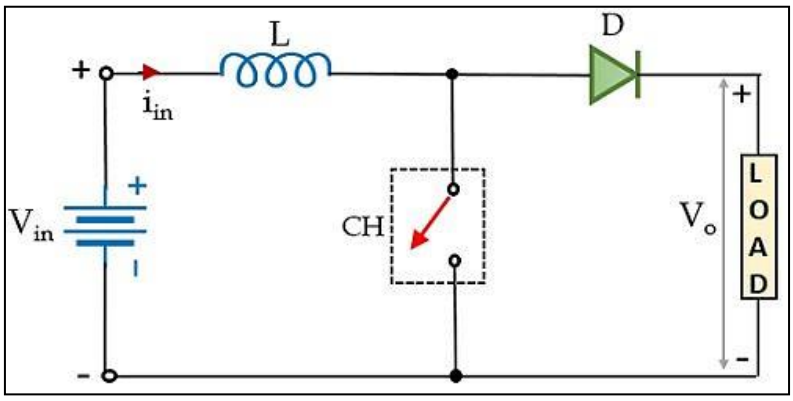

Figure (II.7): Elementary Circuit of Boost Converter

"The circuit presented here represents a fundamental configuration of a step-up DC-DC converter, which necessitates a large inductor (L) connected in series with the voltage source. The overall circuit arrangement functions to ensure the maintenance of a regulated DC output signal."

To comprehend the operation of the given circuit in generating an increased DC signal at the load, consider the initial phase. When the chopper (CH) is in the ON state, the presence of the DC supply input allows current to flow through the closed circuit path, specifically passing through the inductor, as illustrated in the figure below.

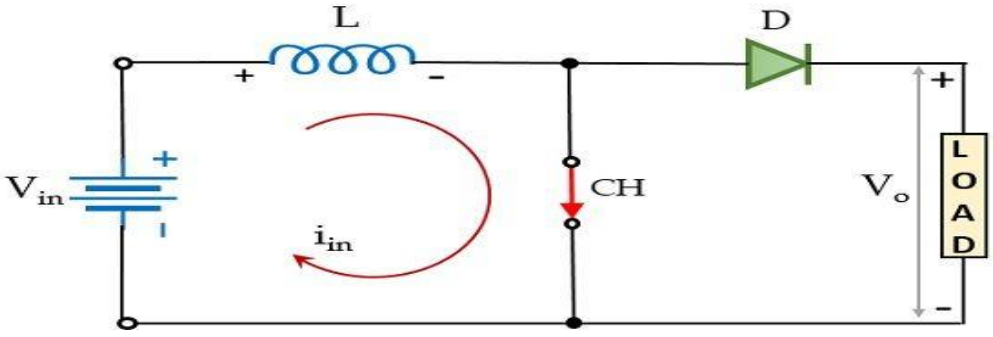

Figure (II.8): The Chopper CH is in on State

"In this configuration, the polarity of the inductor aligns with the direction of current flow. During this phase, the diode remains in a reverse-biased state, preventing current from flowing through that section of the circuit while the DC-DC converter is in the ON state. Consequently, the voltage across the DC-DC converter is directly applied to the load

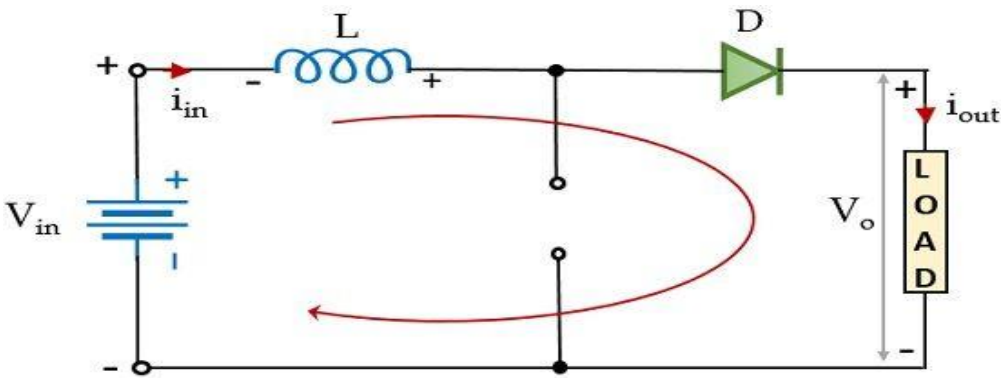

Figure (II.9): The Chopper CH is in Off State

"Furthermore, when the chopper (CH) transitions to the OFF state, the circuit path that previously conducted current becomes inactive. However, since the inductor stores energy in the form of a magnetic field, the current through it does not immediately diminish.

"According to Lenz's law, a reverse current is induced, opposing the change that generated it. Consequently, the polarity of the inductor reverses. This reversed polarity forward-biases the diode within the circuit, allowing current to flow through the diode and reach the load during the chopper's OFF state (T_off). However, it is important to note that the current through the inductor gradually decreases over time and eventually diminishes completely.

Thus, the total voltage across the load will be given as:

$$V_{\text{out}} = V_{\text{in}} + V_L \qquad \text{(II. 25)}$$

This means that the output voltage exceeds the applied input voltage. Thus, performs step-up conversion as the energy stored within the inductor during the T_{on} period is released during the T_{off} period.

During the T_{on} period, the voltage across the inductor will be given as:

$$V_L = L\frac{di}{dt} \qquad (II.26)$$

Let us have a look at the waveform representation of the step-up choppershownbelow:

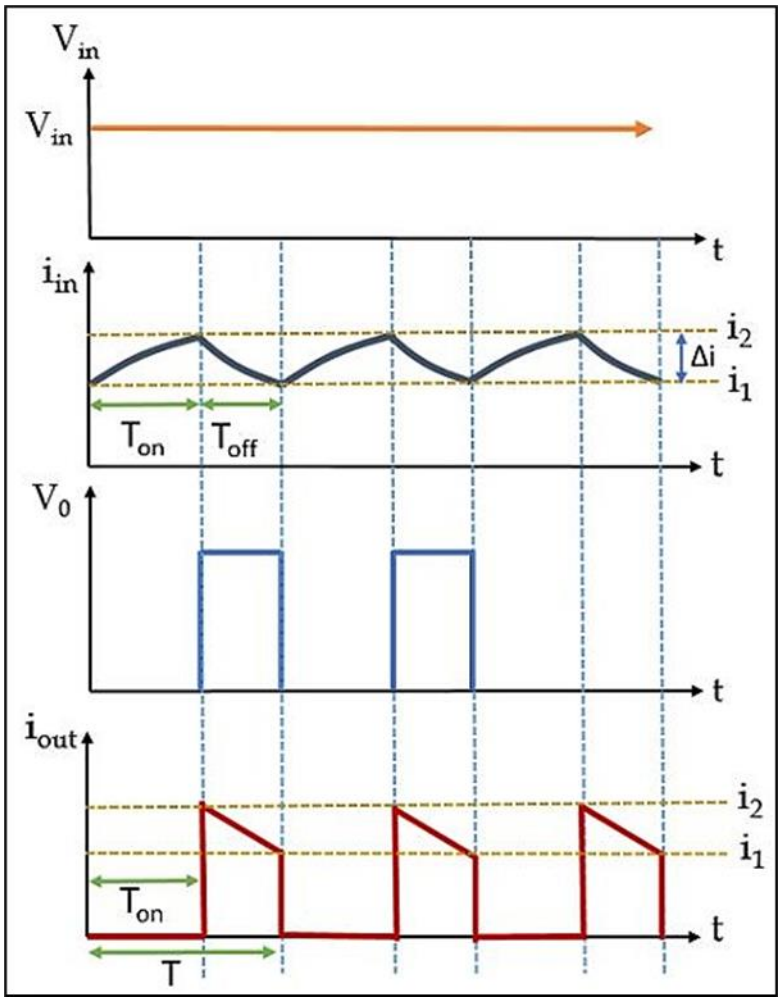

Figure (II.10): Waveform Representation

During the Ton interval, the current flowing through the inductor increases from $\mathbf{i_1}$ to $\mathbf{i_2}$, as clearly illustrated in the figure above. Conversely, during the Toff interval, the inductor current decreases from $\mathbf{i_2}$ to $\mathbf{i_1}$. Regarding the voltage across the inductor, during the turn-on period, it is equivalent to the applied input voltage. However, when the switch **CH** is turned off, applying Kirchhoff's Voltage Law (KVL) to the circuit configuration presented in the figure results in the following equation

$$V_L - V_0 + V_{\text{in}} = 0 \qquad (II.27)$$

This means,

$$V_L = V_0 - V_{\text{in}} \quad \text{(II. 28)}$$

Considering that output current is varying linearly, the energy input provided by the source to the inductor, when CH is on, is given as:

W_{on} = (voltage across the inductor)(average current through the inductor)T_{on}

$$W_{on} = V_{\text{in}} \left(\frac{i_1 + i_2}{2}\right) T_{on} \quad \text{(II. 29)}$$

Further, the energy that the inductor releases to the load when CH is off is given as:

W_{off} = (voltage across the inductor) (average current through the inductor) T_{off}

$$W_{\text{off}} = V_{\text{out}} - V_{\text{in}} \left(\frac{i_1 + i_2}{2}\right) T_{\text{off}} \quad \text{(II. 30)}$$

For a lossless system, comparing the two energies, we will have,

$$V_{\text{in}} \left(\frac{i_1 + i_2}{2}\right) T_{\text{on}} = V_{\text{out}} - V_{\text{in}} \left(\frac{i_1 + i_2}{2}\right) T_{\text{off}} \quad \text{(II. 31)}$$

On simplifying,

$$V_{\text{in}}\, T_{\text{on}} = V_{\text{out}}\, T_{\text{off}} - V_{\text{in}}\, T_{\text{off}} \quad \text{(II. 32)}$$

$$V_{\text{out}}\, T_{\text{off}} = V_{\text{in}}\, T_{\text{on}} + V_{\text{in}}\, T_{\text{off}} \quad \text{(II. 33)}$$

$$V_{\text{out}}\, T_{\text{off}} = V_{\text{in}} (T_{\text{on}} + T_{\text{off}}) \quad \text{(II. 34)}$$

Since we know, $T = T_{\text{on}} + T_{\text{off}}$, therefore,

$$V_{\text{out}}\, T_{\text{off}} = V_{\text{in}}\, T \quad \text{(II. 35)}$$

$$V_{\text{out}} = V_{\text{in}} \frac{T}{T_{\text{off}}} \quad \text{(II. 36)}$$

$$V_{\text{out}} = V_{\text{in}} \frac{T}{T - T_{\text{on}}} \quad \text{(II. 37)}$$

$$V_{\text{out}} = V_{\text{in}} \frac{1}{\left(\frac{T}{T} - \frac{T_{\text{on}}}{T}\right)} \quad \text{(II. 38)}$$

Since, we know, duty cycle i.e., $\alpha = T_{on}/ T$

$$V_{0ut} = V_{\text{in}} \frac{1}{(1-\alpha)} \quad \text{(II. 39)}$$

Thus, we can conclude here that the average load voltage can be stepped up with the change in the duty cycle.

II.4.3. Buck-Boost Converter:

The buck-boost converter is a type of DC-DC converter capable of producing an output voltage magnitude that can be either greater or less than the input voltage magnitude. It is employed to "step up" or "step down" DC voltage, analogous to the function of a transformer in AC circuits. This converter is equivalent to a flyback **converter** but utilizes a single inductor instead of a transformer. Two distinct configurations of buck-boost DC-DC converters, commonly referred to as choppers, include the versatile buck-boost converter, which can operate as either a step-down or step-up converter based on its duty cycle **(**D**)**. A typical buck-boost converter circuit is illustrated below

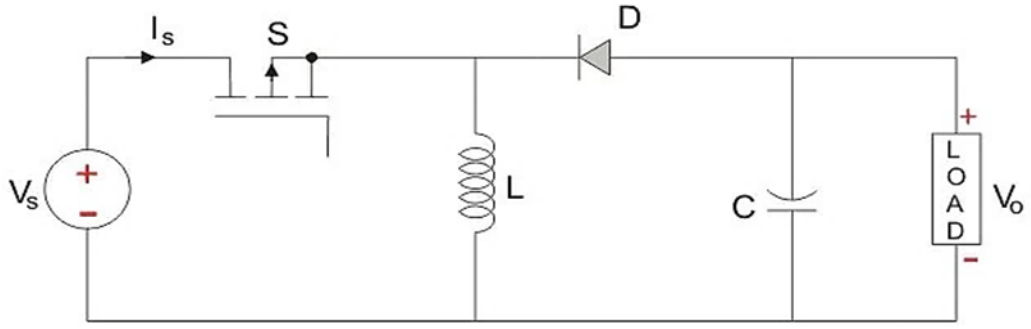

Figure (II.11): The Circuit Representation of Buck-Boost Converter

The input voltage source is connected to a solid-state switching device, while the second switching component is a diode. The diode is oriented in reverse with respect to the direction of power flow from the source

It is connected to both a capacitor and the load, which are arranged in parallel, as illustrated in the figure above

The controlled switch in the converter operates using Pulse Width Modulation **(PWM)** to alternate between on and off states. PWM can be implemented based on either time or frequency, with time-based modulation being the more commonly utilized method

Although frequency-based modulation offers versatility, it has the drawback of requiring a broad range of frequencies to accurately regulate the switch and achieve the desired output voltage.

Time-based modulation is predominantly utilized in DC-DC converters due to its simplicity in design and implementation

In this type of PWM modulation, the frequency remains constant. The buck-boost converter operates in two distinct modes, with the first mode occurring when the switch is in the conducting state.

Mode I: Switch is ON, Diode is OFF

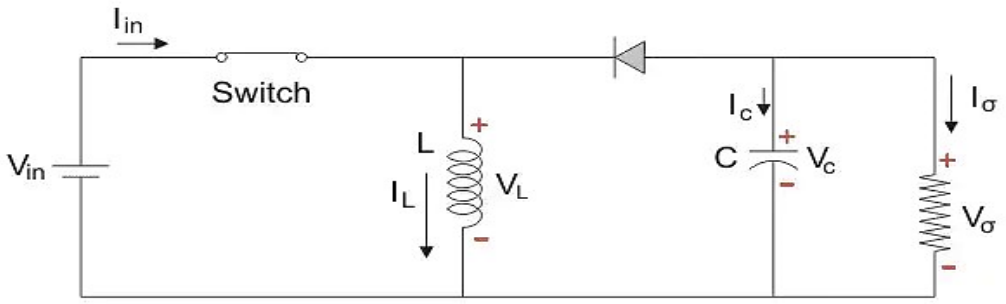

Figure (II.12): The Equivalent Circuit of Mode I

When the switch is in the ON state, it ideally functions as a short circuit, providing zero resistance to the flow of current. Consequently, during this state, the entire current passes through the switch and the inductor, returning to the DC input source

During the ON state of the switch, the inductor stores energy. When the solid-state switch is turned OFF, the polarity of the inductor reverses, allowing current to flow through the load, the diode, and back to the inductor. Consequently, the direction of current through the inductor remains unchanged

Let us say the switch is on for a time T_{ON} and is off for a time T_{OFF}.

We define the time period, T, as:

$$T = T_{ON} + T_{OFF} \quad \text{(II. 40)}$$

and the switching frequency:

$$f_{\text{switching}} = \frac{1}{T} \quad \text{(II. 41)}$$

Let us now define another term, the duty cycle:

$$D = \frac{T_{ON}}{T} \quad \text{(II. 42)}$$

Let us analyse the Buck Boost converter in steady state operation for this mode using KVL.

$$\begin{gathered} V_{in} = V_L \\ V_L = L\frac{di_L}{dt} = V_{in} \\ \frac{di_L}{dt} = \frac{\Delta i_L}{\Delta t} = \frac{\Delta i_L}{DT} = \frac{V_{\text{in}}}{L} \end{gathered} \quad \text{(II. 43)}$$

Since the switch is closed for a time $T_{ON} = DT$ we can say that $\Delta t = DT$.

$$(\Delta i_L)_{\text{closed}} = \left(\frac{V_{in}}{L}\right) DT \quad \text{(II. 44)}$$

While performing the analysis of the Buck-Boost converter we have to keep in mind that

- The inductor current is continuous and this is made possible by selecting an appropriate value of L.

In a steady-state condition, the inductor current increases with a positive slope to a peak value during the ON state and subsequently decreases back to its initial value with a negative slope during the OFF state. As a result, the net change in inductor current over a complete cycle is zero

Mode II: Switch is OFF, Diode is ON

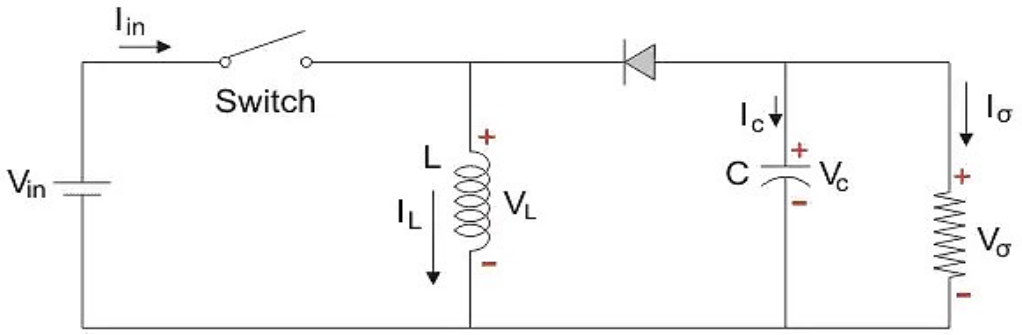

Figure (II.13): The Equivalent Circuitof ModeII

In this operational mode, the polarity of the inductor is reversed, resulting in the release of the energy stored within it, which is ultimately dissipated across the load resistance. This process ensures the continuous flow of current in the same direction through the load while also increasing the output voltage, as the inductor functions as an additional energy source alongside the input source. However, for analytical purposes, the original conventions are maintained to facilitate circuit analysis using Kirchhoff's Voltage Law (KVL)

Buck Boost Converter Formula

Let us now analyse the Buck Boost converter in steady state operation for Mode II using KVL.

$$V_L = V_o \tag{II.45}$$

$$V_L = L\frac{di_L}{dt} = V_o \tag{II.46}$$

$$\frac{di_L}{dt} = \frac{\Delta i_L}{\Delta t} = \frac{\Delta i_L}{(1-D)T} = \frac{V_o}{L} \tag{II.47}$$

Since the switch is open for a time

$$T_{OFF} = T - T_{ON} = T - DT = (1-D)T \tag{II.48}$$

we can say that

$$\Delta t = (1-D)T \tag{II.49}$$

$$(\Delta i_L)_{\text{open}} = \left(\frac{V_o}{L}\right)(1-D)T \tag{II.50}$$

It is already established that the net change of the inductor current over any one complete cycle is zero.

$$(\Delta i_L)_{\text{closed}} + (\Delta i_L)_{\text{open}} = 0 \qquad (\text{II}.51)$$

$$\left(\frac{V_o}{L}\right)(1-D)T + \left(\frac{V_{\text{in}}}{L}\right)DT = 0 \qquad (\text{II}.52)$$

$$\frac{V_o}{V_{\text{in}}} = \frac{-D}{1-D} \qquad (\text{II}.53)$$

We know that D varies between 0 and 1. If D > 0.5,

the output voltage is larger than the input; and if D < 0.5, the output is smaller than the input. But if D = 0.5 the output voltage is equal to the input voltage[24].

II.5. Comparison of Converter Types:

Table (II.1) presents a summary of the voltage gains and switch stresses associated with different types of converters. The variation of voltage gains as a function of the duty cycle is illustrated for these converters. Although several configurations can be classified as boost converters, particularly when the duty cycle exceeds 0.5, only the conventional boost converter maintains voltage boosting capability across the entire duty cycle range. For instance, at a duty cycle of 0.5, the boost converter achieves an output voltage that is twice the input voltage. In contrast, for other boost-derived topologies, the output voltage remains equal to the input voltage at this duty cycle. It is only as the duty cycle approaches 1 that these alternative configurations exhibit behavior similar to that of the conventional boost converter. [25].

Converter /Parameters	Voltage Gain $\frac{Vout}{Vin}$	Voltage Controls $V_{k,max} = \lvert Vd,max \rvert$	Current Controls $i_{k,max} = V_{d,max} = i_{d,max}$
Boost	$\frac{1}{1-\alpha}$	$\frac{Vin}{1-\alpha} + \frac{\Delta \text{Vout}}{2}$	$\frac{Iout}{1-\alpha} + \frac{\Delta \text{IL}}{2}$
Buck	$\frac{\alpha}{1-\alpha}$	$\frac{Vin}{1-\alpha} + \frac{\Delta \text{Vout}}{2}$	$\frac{VC}{1-\alpha} + \frac{\Delta \text{Vout}}{2}$
Buck-Boost	α	Vin	$i_{L} + \frac{\Delta \text{IL}}{2}$

Table (II.1): Comparison of Converter Types.

II.6. Efficiency of Static Converters:

The table provides insight into the efficiency of some well-known converter types.[26]

Structure	Conversion Efficiency	Battery
Boost	92%	24V
Buck	93%	12V
Buck-Boost	92%	12-24V

Table (II.2): Efficiency of Static Converters.

II.7. Conclusion:

In conclusion, DC-DC converters play a crucial role in modern electronics, facilitating efficient power management by converting one voltage level to another. With various types such as buck, boost, buck-boost. They offer versatility in meeting the diverse voltage requirements of different electronic systems.

These converters find wide-ranging applications in industries such as automotive, renewable energy, telecommunications, and consumer electronics. From powering small electronic devices to managing energy flow in solar power systems, DC-DC converters are indispensable.

On a related note, Maximum Power Point Tracking (MPPT) is a vital technology, particularly in renewable energy systems such as solar power. It enables efficient extraction of maximum power from photovoltaic panels by adjusting the electrical operating point. In the following chapter we will delve into MPPT, its importance, and its various implementation methods.

Chapter III

Maximum Power Point Tracking

III.1. Introduction:

In order to overcome the performance issue of solar panels and achieve maximum efficiency, it is necessary to optimize the design of all parts of the PV system. Additionally, it is essential to optimize the DC/DC converters used as the PV generator input interface and the load in order to extract maximum power continuously and thus operate the PV system at its maximum power point (MPP) without loss in the transferred energy using a Maximum Power Point Tracking (MPPT) controller. Consequently, maximum power is obtained under varying load and atmospheric conditions (brightness and temperature).

A significant number of MPPT control techniques have been developed since the 1970s, starting with simple techniques such as MPPT controllers based on feedback of voltage and current states, to more efficient controllers using algorithms to calculate the PV system's MPP. Among the most commonly used techniques are the Incremental Conductance (INC) method, Perturb and Observe (P&O) method, and "hill climbing" method[27].

III.2. Maximum Power Point Tracking:

The improvement of photovoltaic (PV) system efficiency requires maximizing the power output of the PV generator. This objective can be attained by accurately selecting the operating point, thereby matching the load impedance to the voltage source. The DC-DC converter functions as an impedance adapter, ensuring operation at the optimal point, which facilitates the maximum power extract [28]**.**

Maximizing the power output of a photovoltaic (PV) source requires identifying the optimal operating point. This process, known as maximum power point tracking (MPPT), relies on iterative search algorithms to determine the operating point of the solar module, ensuring maximum power generation without disrupting system operation. MPPT techniques are designed to continuously optimize the power extracted from PV modules. The extracted power is calculated based on current and voltage measurements of the module, obtained through the multiplication of these two quantities. Various MPPT methods utilize these measurements to track the true maximum power point (MPP). Several MPPT control techniques exist, among which we outline the principles of a few, including the constant voltage method, the constant

current method, the incremental conductance algorithm, and the perturbation and observation method. The latter is employed in this study due to its simplicity and ease of implementation.

III.3. Working principle of MPPT:

Specific control laws are designed to enable devices to operate at their maximum characteristic points without prior knowledge of these points, the timing of their modifications, or the reasons for such changes. In the context of energy sources, this corresponds to identifying maximum power points. This type of control is commonly referred to in the literature as Maximum Power Point Tracking (MPPT). The fundamental principle of MPPT techniques is to continuously search for the maximum power point (MPP) while ensuring optimal adaptation between the generator and its load, thereby facilitating the transfer of maximum power.[29].

To simplify the operating conditions of this control, a DC load is selected. Within this system, MPPT control is inherently associated with a four-pole network that possesses degrees of freedom, enabling adaptation between the PV generator and the load. In the context of solar energy conversion, this four-pole network can be implemented using a DC-DC converter, ensuring that the power supplied by the PV generator corresponds to the maximum power **(**P_MAX**)** it generates, thereby allowing for its direct transfer to the load.

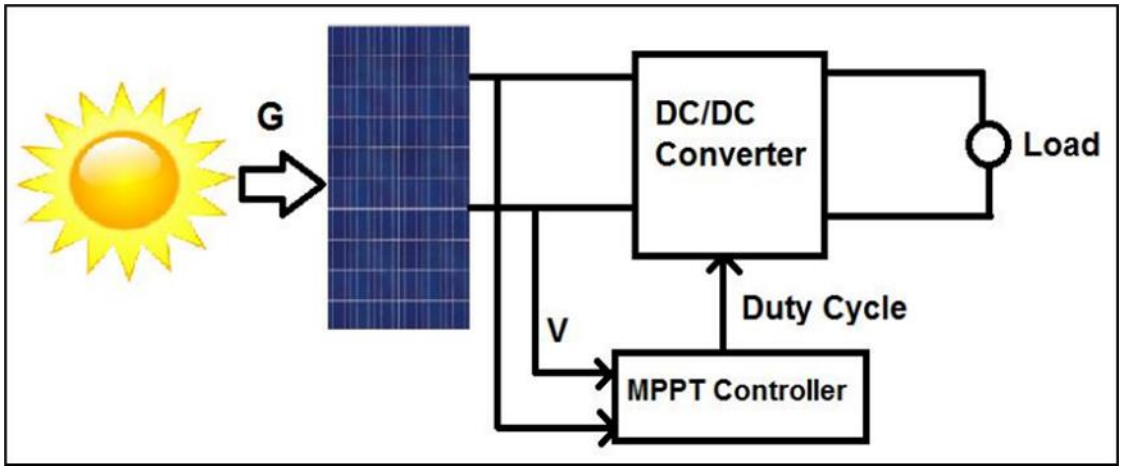

Figure (III.1): Block Diagram of The PV System

The commonly employed control technique involves automatically adjusting the duty cycle to maintain the generator at its optimal operating point, accounting for

sudden load variations that may occur at any time. **Figure (III.2)** illustrates three types of disturbances. Depending on the nature of the disturbance, the operating point shifts from the maximum power point (**MPP1**) to a new operating point (**P1**), which may be located at varying distances from the optimum.

In the case of solar irradiance variation (**case a**), it is necessary to adjust the duty cycle to converge toward the new **MPP2**. For a load variation (**case b**), the operating point shifts, but an appropriate control action can enable the system to reach a new optimal position. To a lesser extent, a third type of operating point variation can occur due to changes in the photovoltaic module's operating temperature (**case c**). While adjustments at the control level are required in this case, the time constraints associated with temperature variations are less critical compared to those in the first two cases.[30].

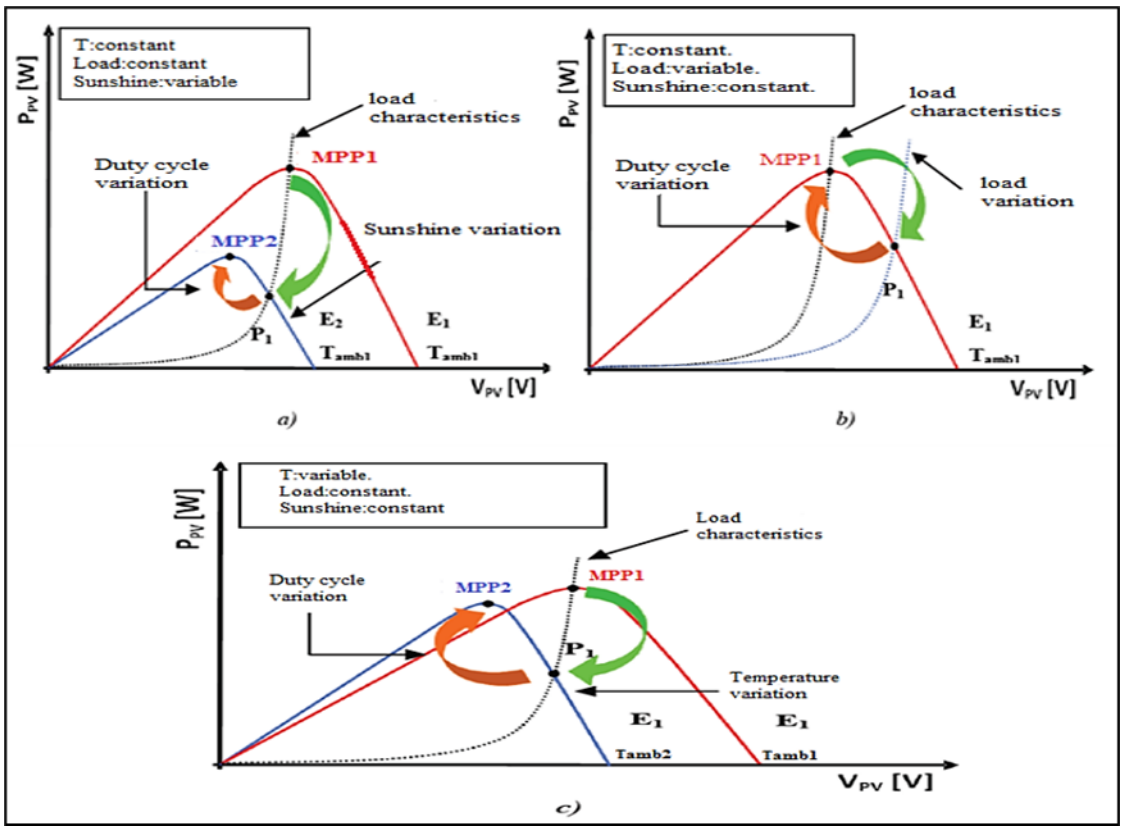

Figure (III.2): Search and Recovery Of MPP

III.4. Classification of MPPT Control:

We can generally classify MPPT controllers according to the type of electronic implementation: analogical, digital, or mixed. However, it is more interesting to

classify them according to the type of search they perform and the input parameters of the MPPT controller.

III.4.1. Classification of MPPT Controllers Based on Input Parameters:

a) MPPT Controllers Operating from Input Parameters:

Several MPPT controllers are designed to track the maximum power point (MPP) by analyzing the evolution of the power output from the PV array. Notable examples include the Perturb and Observe (P&O) method and incremental conductance algorithms, both of which utilize the power supplied by the PV array to implement appropriate control actions for MPP tracking. Additionally, some controllers operate based on proportional relationships between the optimal parameters defining the maximum power point (V_opt and I_opt) and the characteristic parameters of the PV module (V_oc and I_sc)

Notably, MPPT controllers based on neural network methodologies belong to this category. These controllers either utilize extensive computational memory systems to store all possible scenarios or rely on approximation techniques. A key advantage of these controllers is their high precision and rapid response time.[31].

b) MPPT Controllers Operating from Output Parameters of theConverter:

In the literature, there also exist algorithms that utilize the output parameters of DC-DC converters for MPPT control. For instance, some controllers operate by maximizing the output current, a technique primarily employed when the load is a battery. In all systems that rely on output parameters, an approximation of P_max is derived based on the efficiency of the converter. In summary, the higher the efficiency of the conversion stage, the more accurate this approximation becomes. However, in general, all single-sensor systems inherently lack precision. Notably, many of these systems were initially developed for space applications.[31].

III.4.2. Classification of MPPT Controllers According to the Type of Search:

a) Indirect MPPT:

This type of MPPT control leverages the existing relationship between the measured variables, such as VocV_{oc}, which can be easily determined, and the

approximate location of the MPP. Additionally, it includes control strategies based on estimating the operating point of the PV system using a predefined parametric model. Some control approaches also achieve optimal voltage tracking by considering only variations in cell temperature, as measured by a dedicated sensor. These control methods offer the advantage of simplicity in implementation and are primarily designed for cost-effective and less precise systems operating in regions with minimal climatic variability.[32].

b) Direct MPPT:

This type of MPPT control determines the optimal operating point (MPP) by analyzing the currents, voltages, or power levels measured within the system, allowing it to respond effectively to unpredictable changes in PV system operation. These methods are generally based on search algorithms that identify the maximum power point of the curve without interrupting system functionality. This is achieved by incrementally adjusting the operating point voltage at regular intervals. If the output power increases, the search direction is maintained for the next step; otherwise, it is reversed. Consequently, the actual operating point oscillates around the MPP.

This fundamental principle can be preserved through alternative algorithms designed to mitigate interpretation errors, which may arise, for instance, due to an incorrect search direction caused by a rapid increase in power resulting from sudden fluctuations in solar irradiance. Determining the power output of the PV generator—critical for identifying the MPP—requires measuring both the generator's voltage and current and computing their product. Additionally, some algorithms introduce small-signal sinusoidal variations in the converter switching frequency to compare the alternating and direct components of the PV system voltage, thereby positioning the operating point as close as possible to the MPP. The primary advantages of this control approach are its high precision and rapid response time[32].

III.5. Different MPPT Commands Synthesis:

Various works on MPPT commands appear regularly in the literature since 1968, the date of publication of the first command law adapted to renewable energy (photovoltaic). Given the large number of publications in this field, we have a classification of different MPPT according to their basic principles.

III.5.1. First MPPT Commands Types:

The algorithm implemented in the initial MPPT control was relatively simple. This was primarily due to the limited computational capacity of microcontrollers available at the time, as well as the fewer constraints related to temperature and solar irradiation, particularly in space applications. The first MPPT control applied to a photovoltaic system was introduced by A.F. Boehringer and was based on an adaptive control algorithm designed to maintain the system at its maximum power point (MPP). This approach, illustrated in Figure 3, can be easily implemented on a computer. The system calculates the power at time $\mathbf{t_i}$ using measurements of I_PV and V_PV, then compares it with the previously stored value from time t_{i-1}. Based on this comparison, a new duty cycle (D) is determined and applied to the static converter

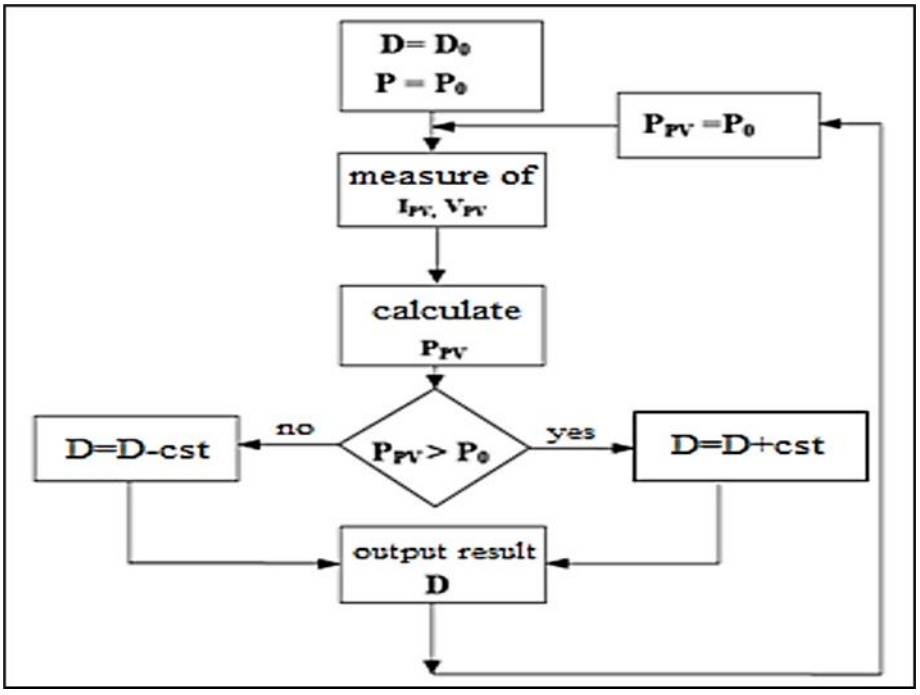

Figure (III.3): Bloc Diagram of a Digital MPPT Command

This principle is always valid from a theoretical point of view and applied nowadays to more efficient numerical algorithms. However, the response time has been improved as well as the PPM search accuracy[30].

III.5.2. Efficient MPPT Commands Algorithms:

The three (04) methods most commonly encountered are commonly referred to respectively as Hill Climbing, Perturb & Observe and Incremental Conductance andArtificial Neural Networks.

III.5.2.1. AlgorithmPerturb and Observe (P&O):

The principle of MPPT control based on the Perturb and Observe (P&O) method involves introducing a small perturbation in the PV voltage (V_PV) around its initial value and analyzing the resulting variation in power (P_PV**).** As illustrated in Figure (III.4)**,** if a positive increment in V_PV leads to an increase in P_PV, this indicates that the operating point is positioned to the left of the MPP. Conversely, if the power decreases following the voltage increment, it suggests that the system has surpassed the MPP

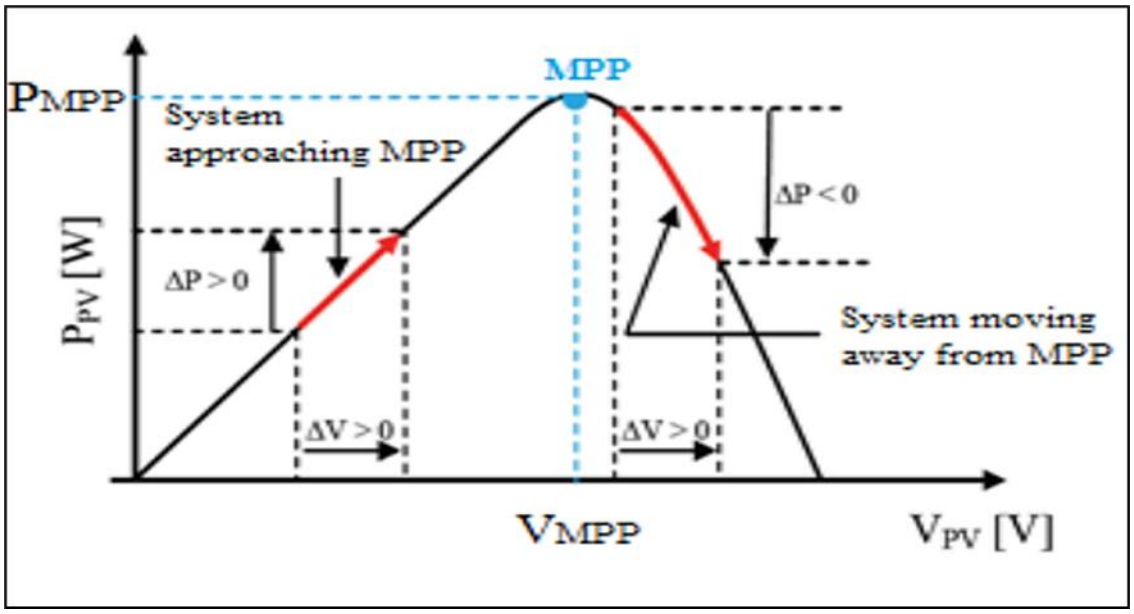

Figure (III.4): Ppv VS VpvCharacteristic of a Solar Panel

Figure (III.5**)** illustrates the algorithm associated with a conventional MPPT control based on the Perturb and Observe (P&O**)** method, in which power variations are analyzed following each voltage perturbation. This control approach requires two sensors—one for current and one for voltage—to determine the power output of the solar generator at every instant. The P&O method is widely utilized today due to its simplicity and ease of implementation. However, it presents certain drawbacks,

particularly the oscillations around the MPP in steady-state operation. Since the MPP search process is conducted periodically, the system continuously oscillates around the MPP, which can lead to efficiency losses..

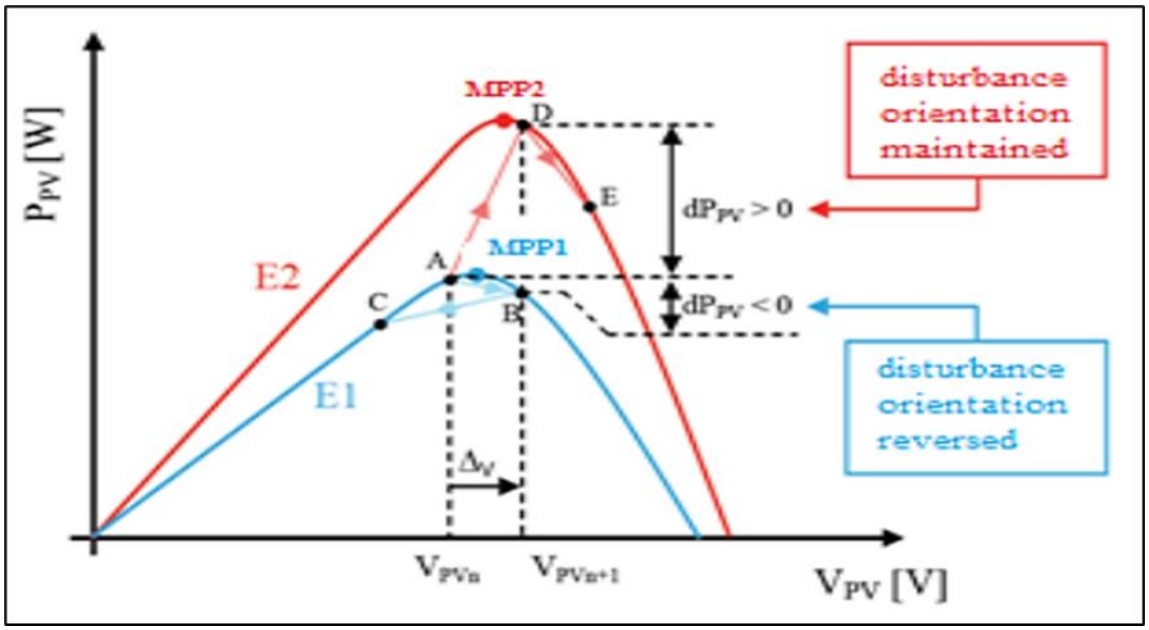

Figure (III.5): Divergence of The P & O Command Due to Radiation Variations

Figure (III.6) shows a detailed algorithm of the P & O command.

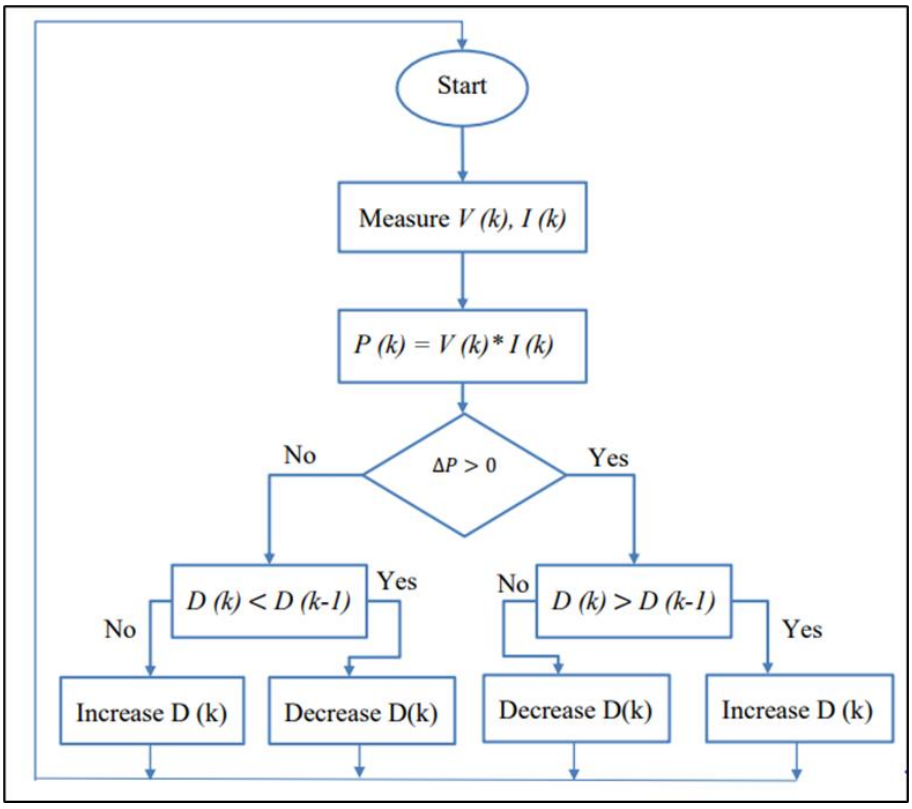

Figure (III.6): Algorithm of The P & O Type of Command

To illustrate this concept, consider the case of a given solar irradiation level, E_1, with an initial operating point at A. Following a voltage perturbation of magnitude ΔV, the operating point shifts to B, indicating a variation in operation without a change in irradiation. This leads to a reversal in the sign of the perturbation, as the negative derivative of power is detected, ultimately resulting in oscillations around the MPP due to the movement of the operating point between B and C. It is important to note that power transfer losses will vary depending on the relative positions of points B and C with respect to A. When the module's irradiation level changes from E_1 to E_2, the operating point transitions from A to D, which in this case is interpreted as a positive power variation[30].

The primary advantage of the hill-climbing MPPT method lies in its simplicity. This approach utilizes the duty cycle of the boost converter as a feedback parameter during the MPPT process [33],[34]**.** However, a key limitation of this technique arises from the trade-off between system stability during periods of constant irradiation and the method's responsiveness to sudden changes in solar radiation [33],[34]**.**

During steady irradiation conditions, a minimal variation in the duty cycle (ΔD) is required to prevent excessive power oscillations around the maximum power point (MPP), which would otherwise reduce the energy harvested by the photovoltaic (PV) system. Conversely, under rapidly changing irradiation conditions, a larger duty cycle variation is necessary to accelerate the tracking of the MPP and enhance system responsiveness.

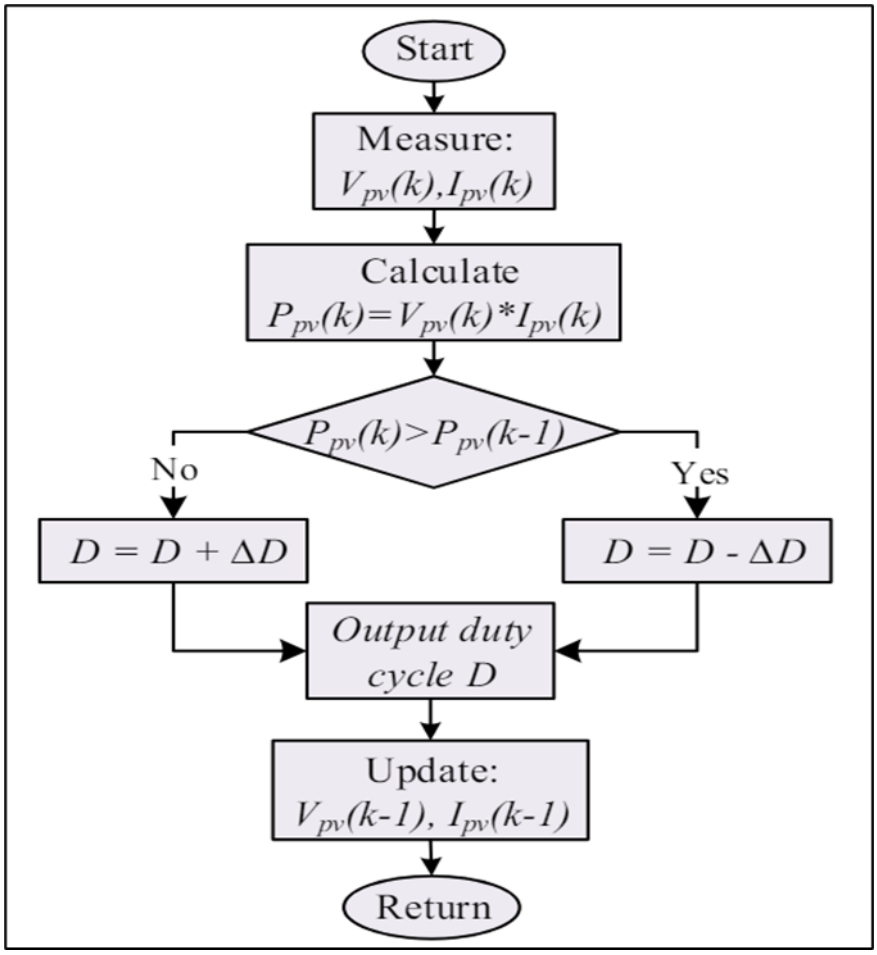

Figure (III.7): State Flowchart of Hill Climbing MPPT Technique.

III.5.2.2. Algorithm Incremental conductance (INC):

The principle of this algorithm is based on utilizing the conductance value (G = I/V) and its incremental change (dG) to determine the position of the operating point relative to the maximum power point (MPP). If the conductance increment (dG) is greater than the negative of the conductance (-G), the duty cycle is decreased. Conversely, if the conductance increment is less than the negative of the conductance, the duty cycle is increased. This iterative process continues until the MPP is accurately reached.[35].

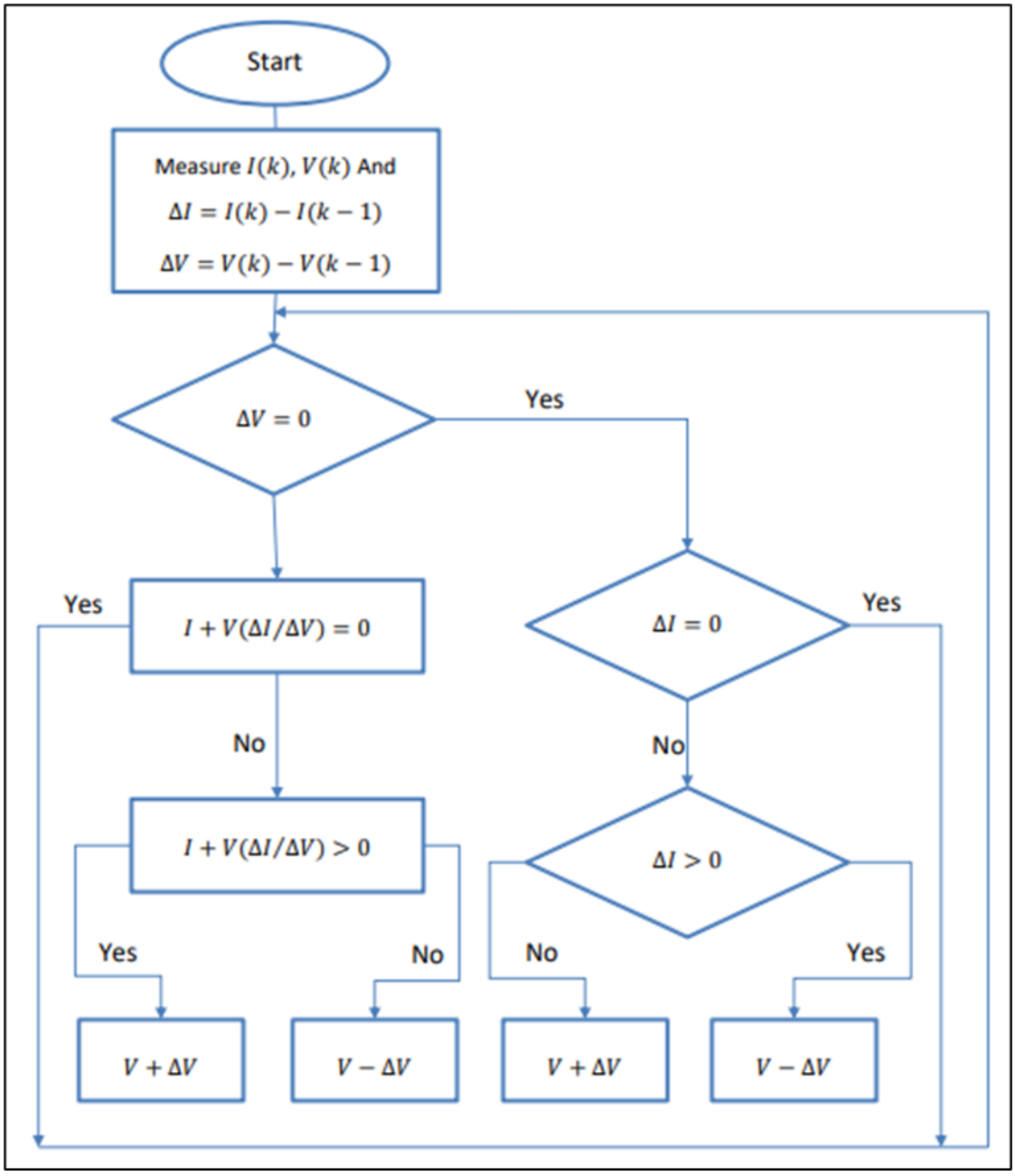

Figure (III.8): Flowchart for The Incremental Conductance Algorithm.

III.5.2.3. Artificial Neural Networks (ANN):

An artificial neural network (ANN**)** typically consists of multiple processors operating in parallel and organized into distinct layers. The input layer receives raw data, analogous to the way the optic nerves process visual information in humans. Subsequently, each intermediate layer processes the outputs from the preceding layer, mimicking the way neurons transmit signals through interconnected pathways in the

human brain. Finally, the output layer produces the system's ultimate results, representing the network's final decision or prediction.

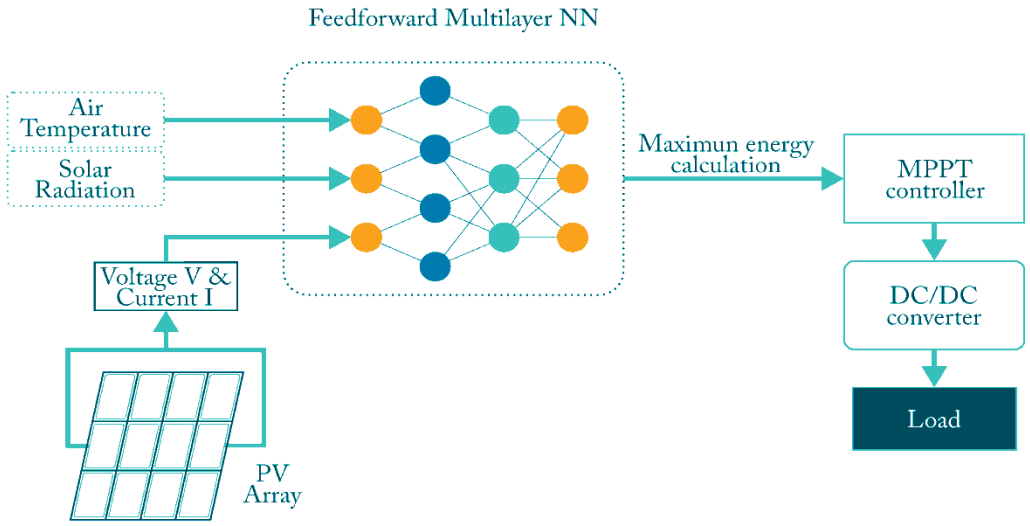

Figure (III.9): Functioning of Artificial Neural Networks

Neural networks enable computers to learn from new data through algorithms. Computers with neural networks are trained on labeled example data to learn tasks like object recognition by analyzing patterns in the examples. Unlike traditional algorithms, neural networks cannot be directly programmed - they learn in a similar way to a child's developing brain. There are three main learning methods:

1. **Supervised Learning:** The algorithm trains on labeled data and adjusts until it can achieve the desired output.
2. **Unsupervised Learning:** The network analyzes unlabeled data, with a cost function guiding it towards the desired result by indicating deviations.
3. **Reinforcement Learning:** The network is rewarded for positive results and penalized for negative ones, enabling it to learn and improve over time like humans learn from mistakes.

III.5.2.3.1. Application of Artificial Neural Networks in MPPT:

Artificial neural networks (ANNs) are utilized to enhance maximum power point tracking (MPPT), a critical component in photovoltaic (PV) systems**.** These networks optimize the efficiency of solar energy capture by dynamically adjusting the operating point of PV panels to ensure maximum power output. This adaptation considers varying environmental factors such as solar radiation levels**,** temperature,

and shading conditions**.** By continuously refining the tracking process, neural network-based MPPT enables PV systems to more effectively harness solar energy, thereby increasing overall energy production.

This example demonstrates the practical application of artificial neural networks (ANNs) and highlights their essential role in enhancing the performance of PV systems through MPPT algorithms.[36].

III.5.2.3.2. Implementation of ANN in MATLAB /SIMULINK :

The Neural Network Fittin g**a**ppli**c**ation in MATLAB offers an intuitive and user-friendly interface for the design, training, and evaluation of artificial neural networks (ANNs)**.** The process involves data selection, network architecture configuration, training, and performance assessment using various plots and metrics**.** This tool is particularly valuable for applications such as maximum power point tracking (MPPT), where precise modeling of complex relationships between inputs and outputs is essential for optimizing system performance

a. Data Collection:

The initial phase of the proposed methodology entails collecting data from MPPT method simulations conducted under diverse operating scenarios. This data collection process serves as the foundation for both training and evaluating the ANN-based MPPT model, ensuring its accuracy and effectiveness in optimizing power extraction.[36].

b. Setting Up the Neural Network Fitting Tool:

To initiate the implementation process, the Neural Network Fitting Tool in MATLAB will be accessed. This tool offers an intuitive interface for the training and evaluation of neural networks. The defined variables will be imported, and the tool will be configured to align with the specific requirements of the application[37].

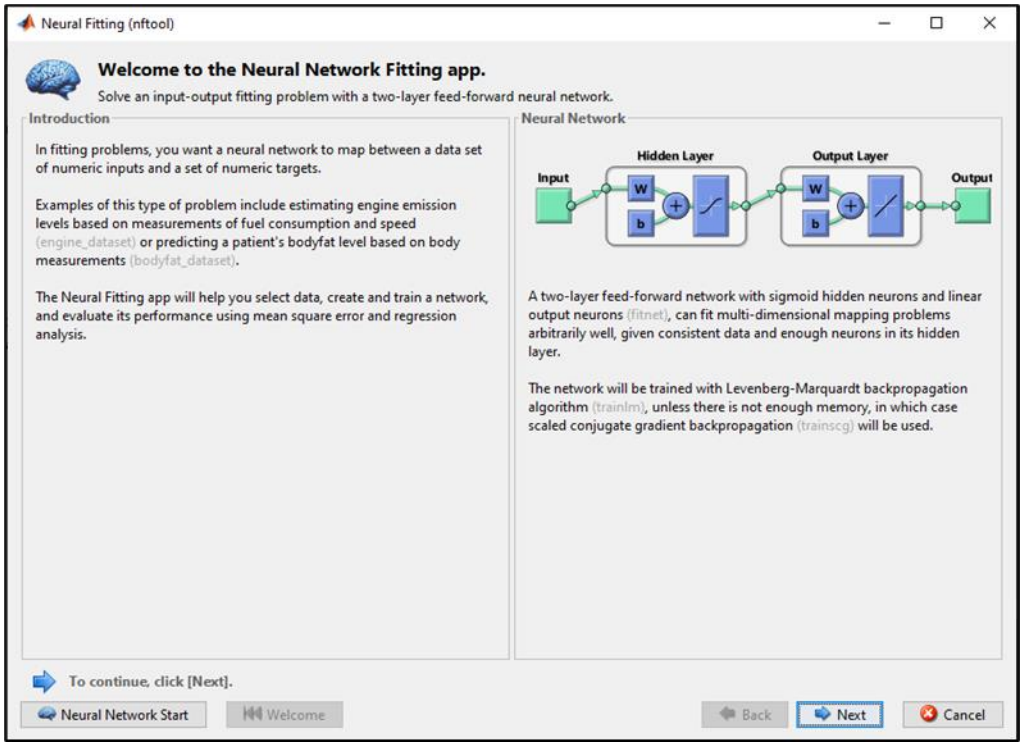

Figure (III.10): Setting Up the Neural Network Fitting Tool

This figure presents the Neural Network Fitting application, outlining its primary purpose of addressing an input-output fitting problem through the implementation of a two-layer feed-forward neural network..

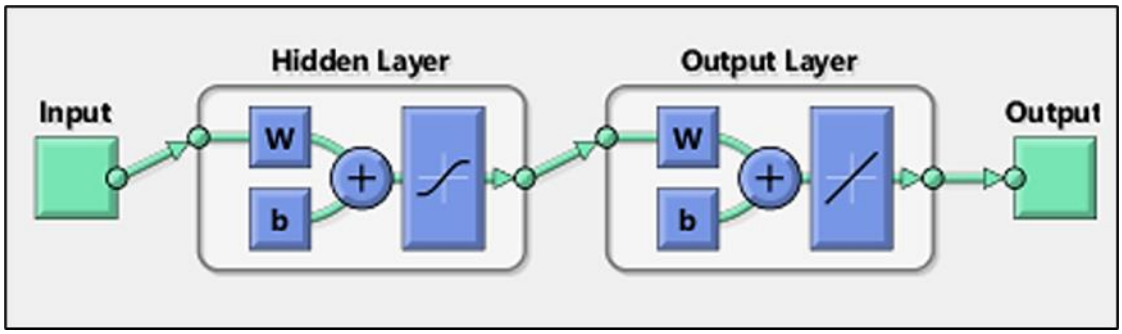

Figure (III.11): Neural Network Structure

The diagram illustrates the **a**rchitecture of the neural network, comprising an input layer, one or more hidden layers**,** and an output layer.

Training Algorithm: The network is trained using the Levenberg-Marquardt backpropagation algorithm (trainlm), which enhances convergence efficiency and accuracy.

c. Select Data:

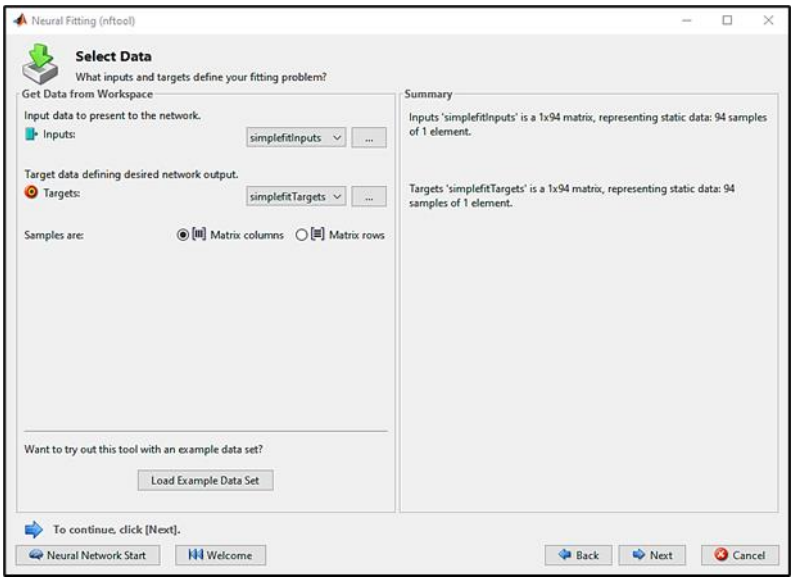

Figure (III.12): Select Data

Inputs and Targets: This figure enables the selection of input and target data from the MATLAB workspace for network training and evaluation.

Data Summary: The summary panel on the right displays the dimensions of the selected dataset. In this instance, 'simplefitInputs' and 'simplefitTargets' serve as example datasets, each consisting of 94 samples.

d. Import Data:

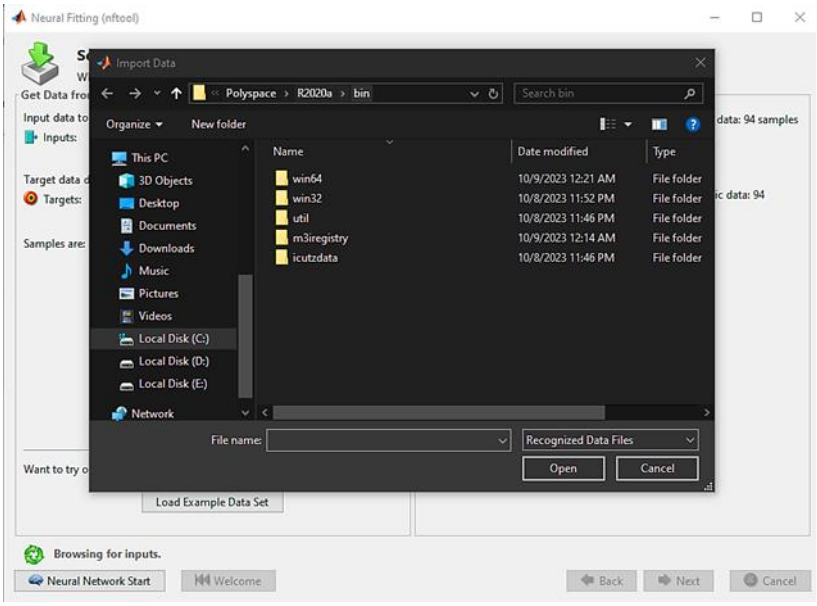

Figure (III.13): Import Data

Data Import: **:** In cases where the data is not already available in the MATLAB workspace, this process enables users to browse and import data files directly from their computer. This step ensures that both the input and target datasets are accurately loaded, facilitating proper network training within the MATLAB

e. Validation and Test Data:

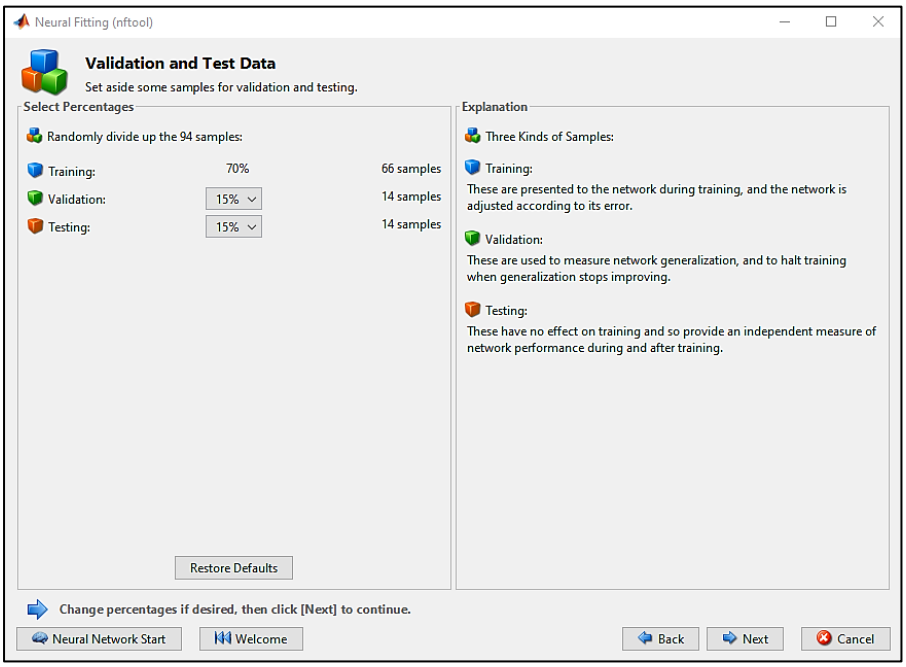

Figure (III.14): Validation and Test Data

Data Division: This figure partitions the dataset into distinct subsets for training, validation, and testing. By default, the allocation consists of 70% for training, 15% for validation, and 15% for testing, ensuring a balanced approach to model development and evaluation.

Explanation: The training dataset is utilized for optimizing the neural network's parameters, while the validation dataset serves to mitigate overfitting by halting training when performance deteriorates. The testing dataset is employed for an independent evaluation of the network's overall performance.

f. Network Architecture:

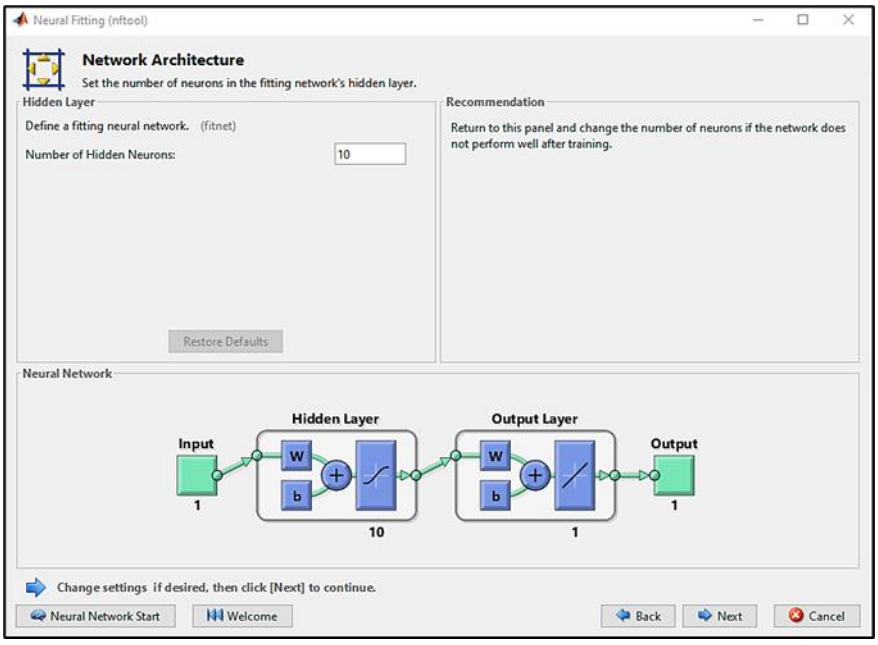

Figure (III.15): Network Architecture

Hidden Layer Configuration: This figure allows you to set the number of neurons in the hidden layer(s). In this example, there are 10 neurons in the hidden layer [37].

Network DiagramThe following diagram provides a visual representation of the neural network architecture, illustrating the designated number of hidden neurons within the structure.

g. Network Training :

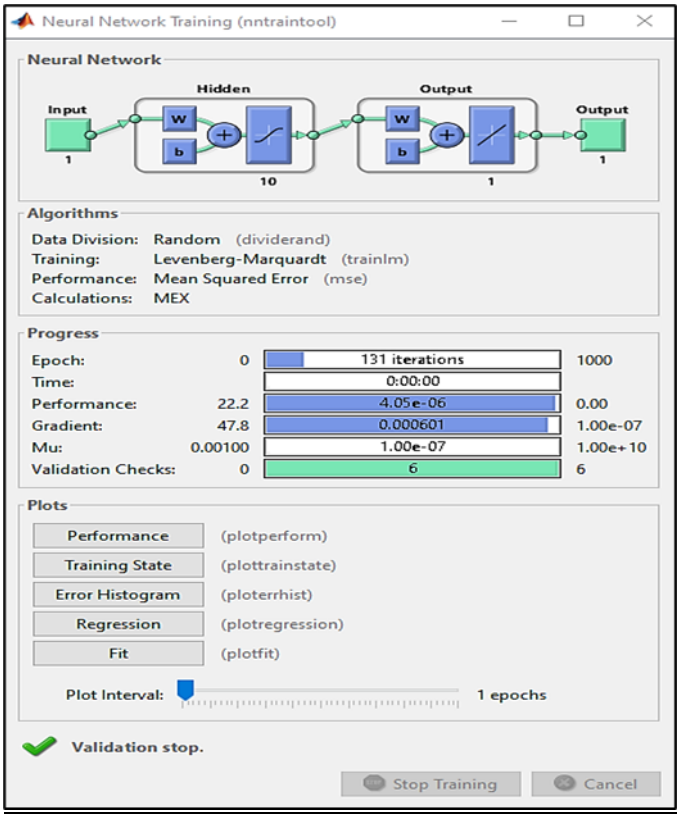

Figure (III.16): Network Training

- Training Process: This figure presents the progression of the neural network training process, detailing key parameters such as the number of epochs, performance metrics, gradient values, and validation checks.
- Performance PlotsSeveral graphical representations are available to track the training process, including performance evaluation plots, training state indicators, error histograms, and regression analysis plots..
- Stop Training: You can manually stop the training process if needed[38].

h. Train Network:

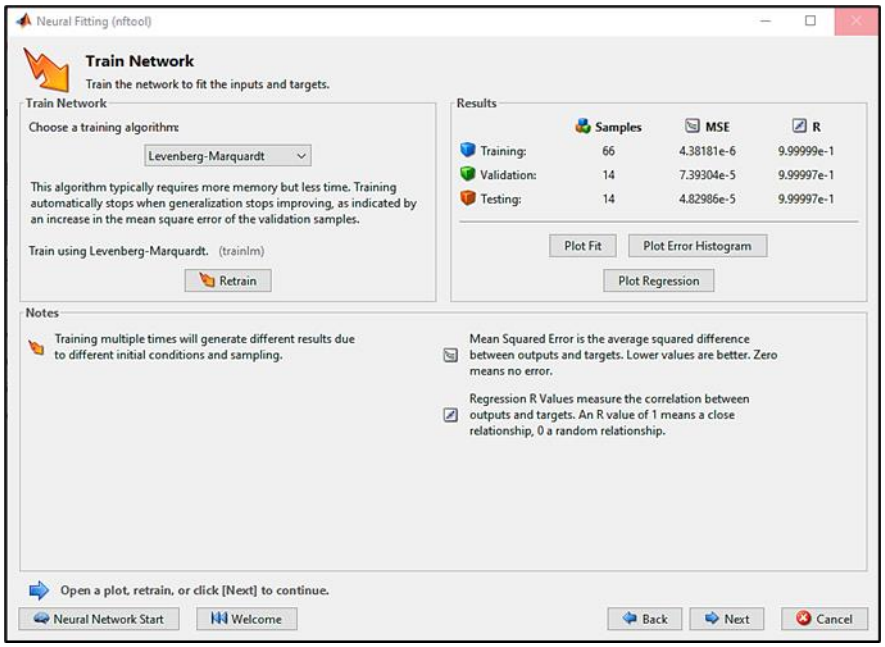

Figure (III.17): Train Network

- Training Results: Upon completion of the training process, this figure presents the results, including the mean squared error (MSE) for the training, validation, and testing datasets
- Regression Plot: This plot illustrates the correlation between the network's outputs and the target values. An R-value approaching 1 signifies a strong fit, indicating the network's ability to accurately model the underlying relationships within the data.
- Error Histogram: This plot shows the distribution of errors between the network outputs and the targets [38].

III.6. Conclusion:

In this chapter, we have initiated the most critical and intricate aspect of this study, which involves presenting the principles underlying the search for the maximum power point (MPP) while outlining the various classifications of MPPT control techniques. A comprehensive analysis of the most frequently encountered MPPT methods in the literature has been provided. The presence of multiple MPPT control strategies underscores the continuous advancement of research in this domain and highlights the challenge of identifying a single, universally applicable solution.

Chapter IV

Simulation Results

IV.1. Introduction:

In this chapter, a comprehensive evaluation and comparative analysis of three widely utilized Maximum Power Point Tracking (MPPT) algorithms— Perturb and Observe (P&O), Incremental Conductance (INC), and Artificial Neural Network (ANN)—is conducted. These algorithms are integral to enhancing the power output of photovoltaic (PV) systems by dynamically adjusting the operating point to ensure optimal energy extraction from solar modules. Accurate tracking of the maximum power point significantly contributes to the overall efficiency and energy yield of PV installations. The P&O method operates based on periodic perturbations and subsequent observations to identify the optimal point. In contrast, the INC approach employs the incremental conductance technique to facilitate more refined adjustments. The ANN-based algorithm, leveraging artificial intelligence, is capable of predicting and tracking the maximum power point with a high degree of precision. This analysis seeks to elucidate the advantages and limitations of each method, thereby offering insights into their relative effectiveness under varying operational conditions.

IV.2. Parameters of System Simulation:

The following characteristics of panel and the parameters of boost converter that are used in our system simulation, are shown in the figure and table below:

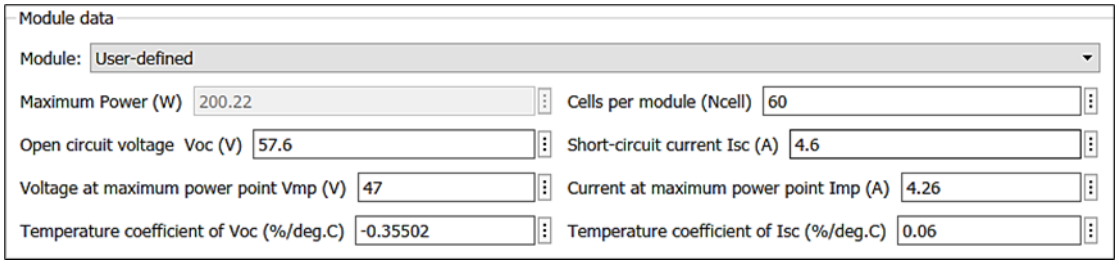

Figure (IV.1): Characteristics of Panel

Boost Converter	Value
Capacitor 1	200 µF
Inductor	3.5 mH
Capacitor 2	100 µF
Resistive Load	300 Ω

Table (IV.1): Parameters of Boost Converter

IV.3. Simulation Results:

IV.3.1. P&O Algorithm:

In this simulation, we used the Perturb and Observe (P&O) algorithm to obtain results for power, voltage, and current. Figure (IV.2) represents the general system simulation, showcasing the overall setup and performance of the P&O -based MPPT system. The figure illustrates the integration of PV panels with the P&O -based MPPT controller, which adjusts the duty cycle to optimize power extraction.

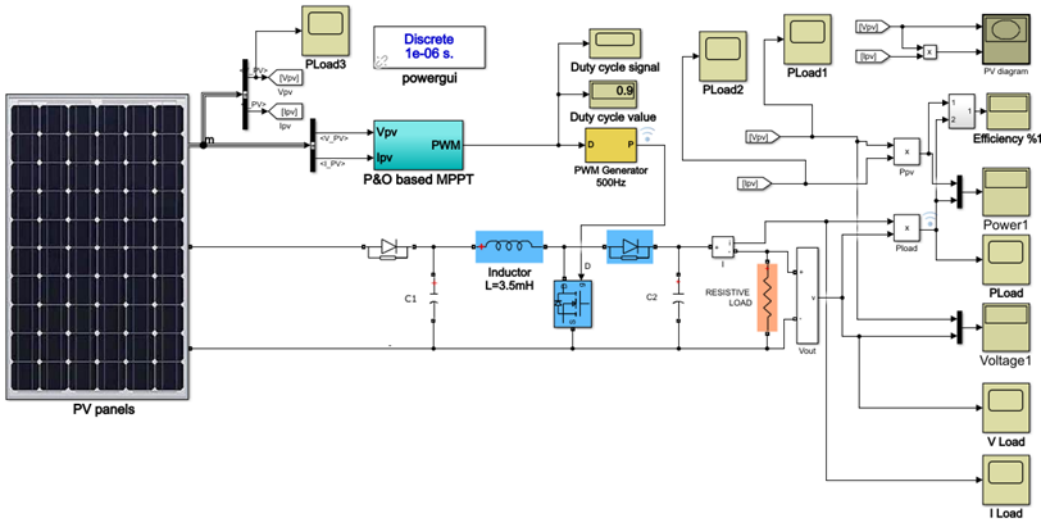

Figure (IV.2): Schema of System Simulation With P&O

a) Constant Irradiance (1000 W/m^2) :

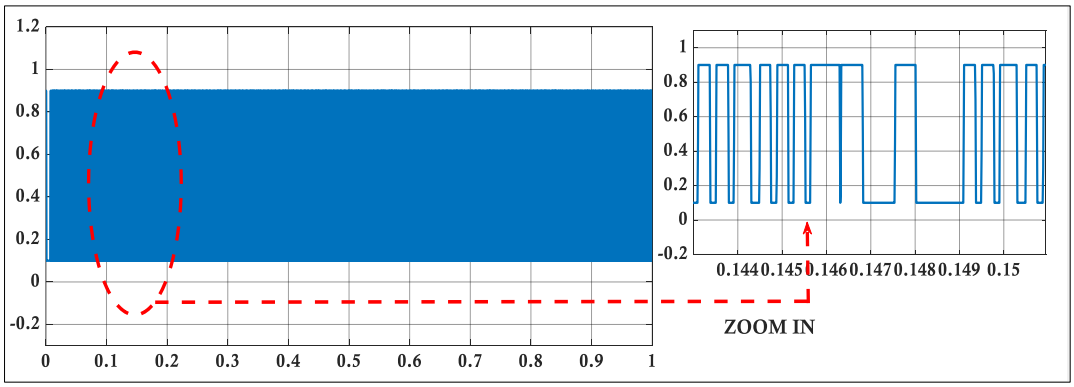

Figure (IV.3): Duty Cycle Simulation Result

The Figure (IV.3) demonstrates the MPPT system's duty cycle behavior, with the main plot showing overall stability and the zoomed-in view revealing critical fluctuations for precise MPPT operation.

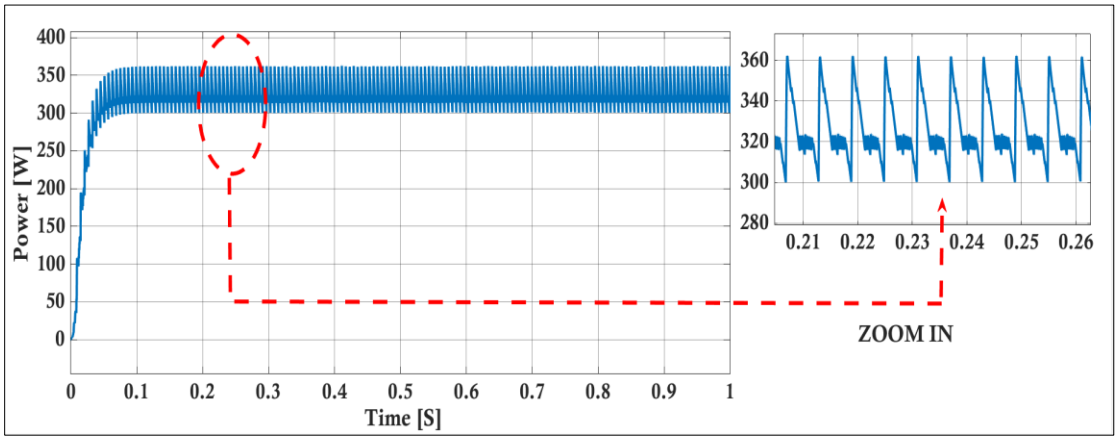

Figure (IV.4): Power Simulation Result

The Figure(IV.4) illustrates the power response of an MPPT system using the P&O algorithm.

The primary plot illustrates a rapid rise in power output, followed by stabilization around 350 W. The magnified view emphasizes the oscillatory behavior inherent to the P&O algorithm, which continuously perturbs the system in its effort to track the maximum power point. These oscillations represent a characteristic trade-off associated with the algorithm's operation, reflecting the balance between dynamic tracking and steady-state accuracy. Understanding this oscillatory pattern is essential for evaluating the efficiency and overall performance of the MPPT system.

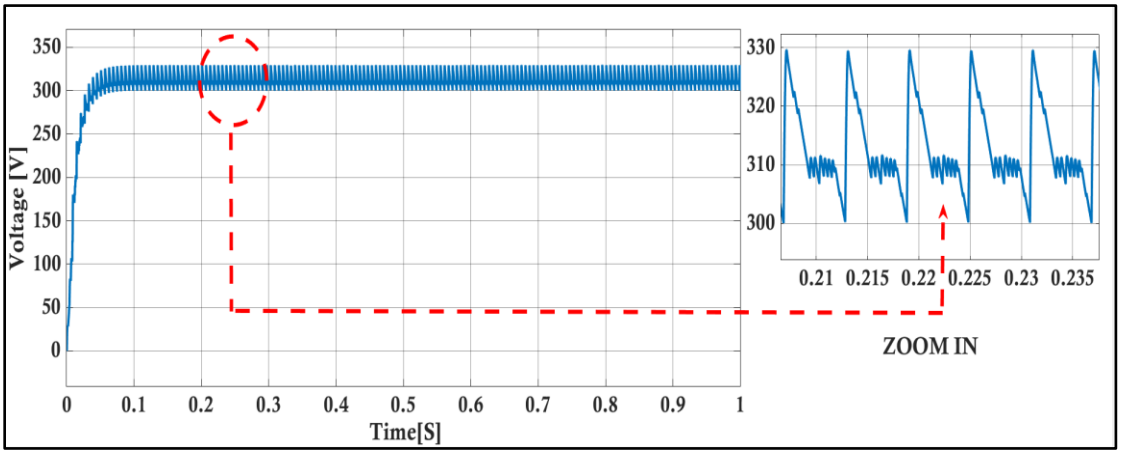

Figure (IV.5): Voltage Simulation Result

The Figure (IV.5) illustrates the voltage response of an MPPT system using the P&O algorithm.

The primary plot depicts a rapid increase in voltage, which subsequently stabilizes at approximately 320 V. The magnified section highlights the oscillatory behavior of the voltage output, reflecting the system's dynamic response during the tracking process

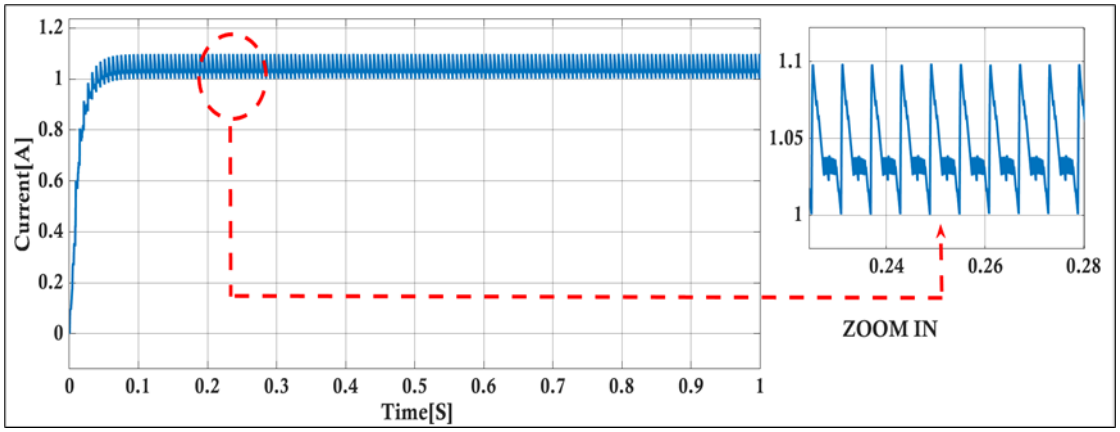

Figure (IV.6): Current Simulation Result

Figure (IV.6) illustrates the current response of a Maximum Power Point Tracking (MPPT) system employing the Perturb and Observe (P&O) algorithm.

The main plot demonstrates a rapid transient response, culminating in stabilization at approximately 1.05 A, indicating that the system has reached the maximum power point. The zoomed-in view offers a detailed perspective of the inherent oscillations around this steady-state value, which are characteristic of the P&O method.

b) Variable Irradiances (1000,800,600, 400 W/m^2):

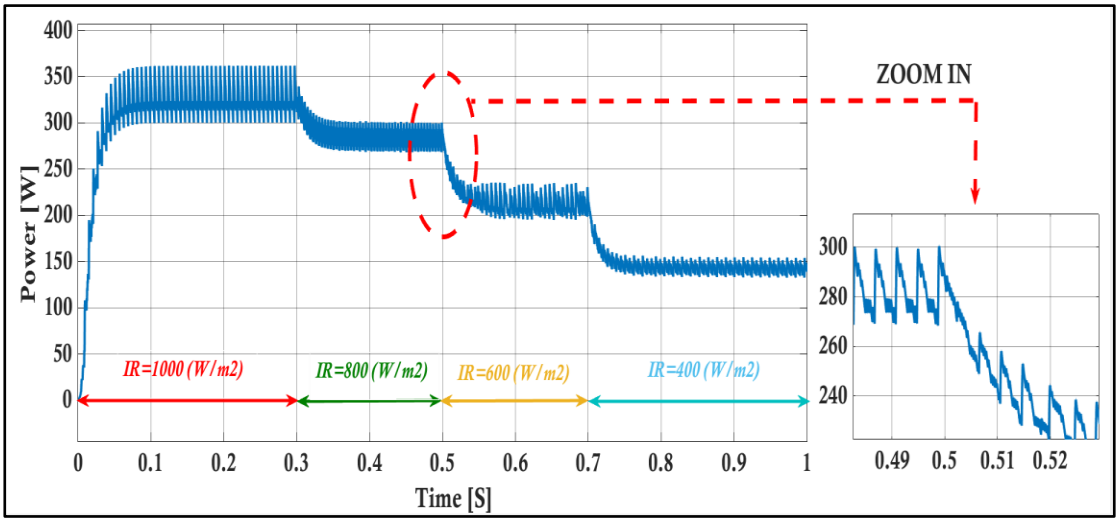

Figure (IV.7): Power Simulation Result

Figure (Ⅳ.7) offers a comprehensive depiction of the power output characteristics of the MPPT system under varying levels of solar irradiance.

The main plot illustrates the system's capability to effectively track the maximum power point across different irradiance conditions, Power stabilizes at approximately 350 W, 300 W, 250 W, and 200 W corresponding to irradiance levels of 1000 W/m², 800 W/m², 600 W/m², and 400 W/m², respectively. The red dashed ellipse, along with the zoomed-in view, highlights the system's transient response to a sudden reduction in irradiance, revealing the typical oscillatory behavior as the P&O algorithm re-adjusts to the new maximum power point.

This in-depth analysis emphasizes the MPPT system's efficiency and its capacity to dynamically adapt in real-time solar energy applications.

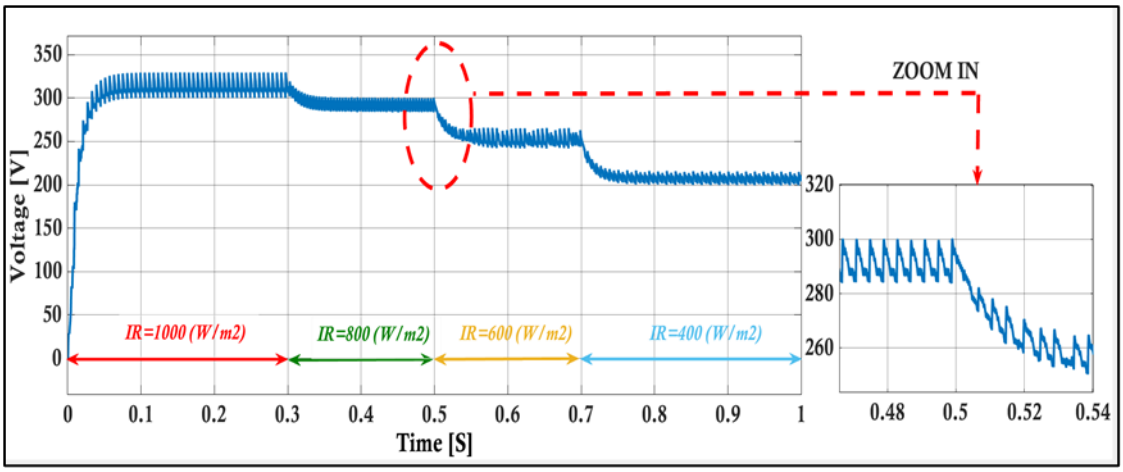

Figure (IV.8): Voltage Simulation Result

Figure (IV.8) illustrates the voltage response of an MPPT system employing the Perturb and Observe (P&O) algorithm under varying irradiance conditions.

The primary plot illustrates the system's rapid stabilization of voltage at approximately 320V, followed by discrete reductions aligned with decreases in irradiance levels. The zoomed-in view provides a detailed depiction of the transient fluctuations, emphasizing the algorithm's ongoing adjustments to maintain optimal operational performance.

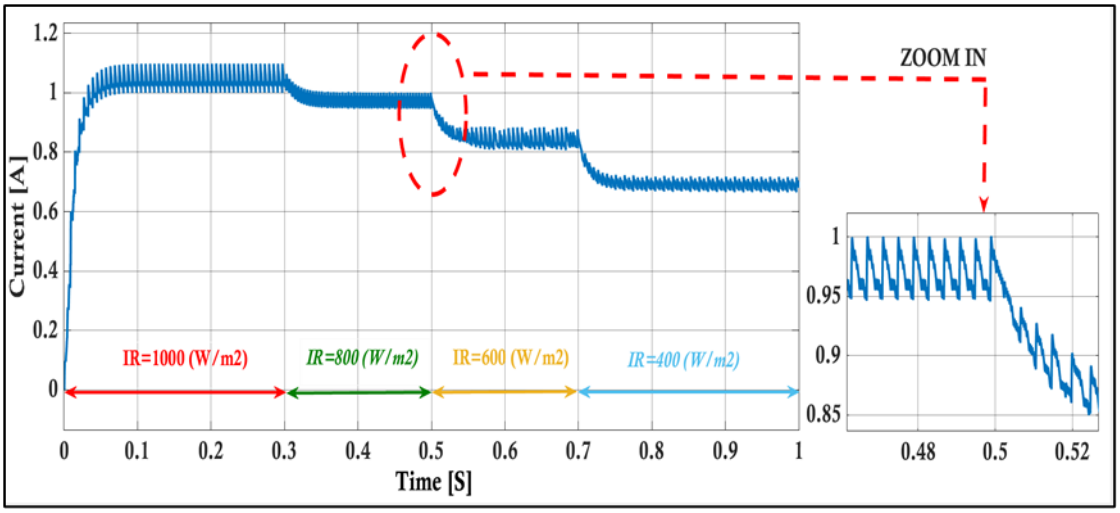

Figure (IV.9): Current Simulation Result

The Figure (IV.9) demonstrates how the MPPT system's current output, managed by the P&O algorithm, adjusts under varying irradiance levels.

The primary plot illustrates the stabilization of the current at approximately 1A, followed by stepwise reductions corresponding to decreases in irradiance levels. The zoomed-in view highlights the transient response during the transition in irradiance

IV.3.2. Incremental Conductance:

In this simulation, we used the Incremental Conductance (INC) algorithm to obtain results for power, voltage, and current. Figure (IV.10)represents the general system simulation, showcasing the overall setup and performance of the INC-based MPPT system. The figure illustrates the integration of PV panels with the INC-based MPPT controller, which adjusts the duty cycle to optimize power extraction.

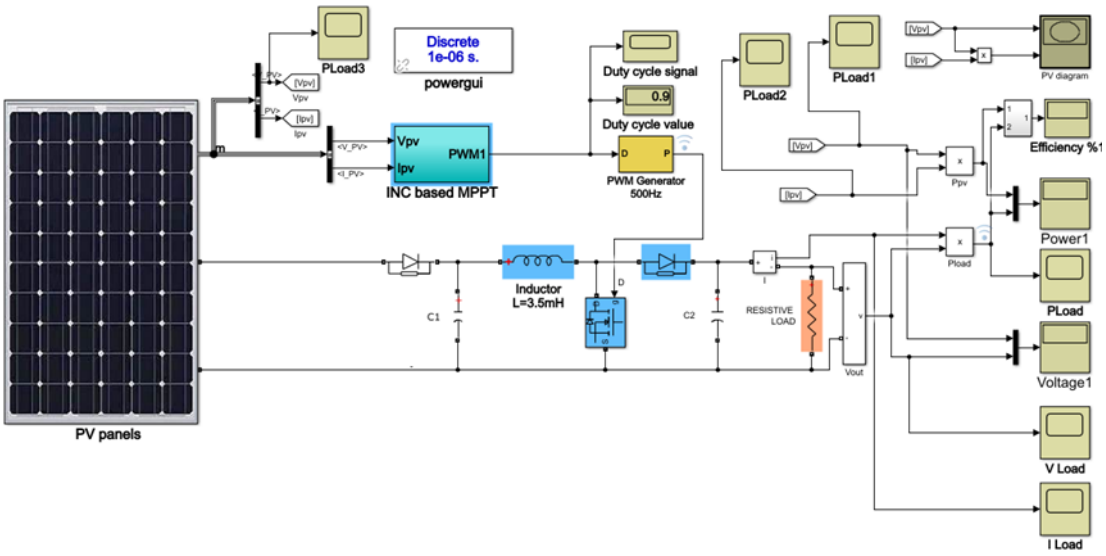

Figure (IV.10): Schema of System Simulation With INC

a) Constant Irradiance (1000 W/m^2):

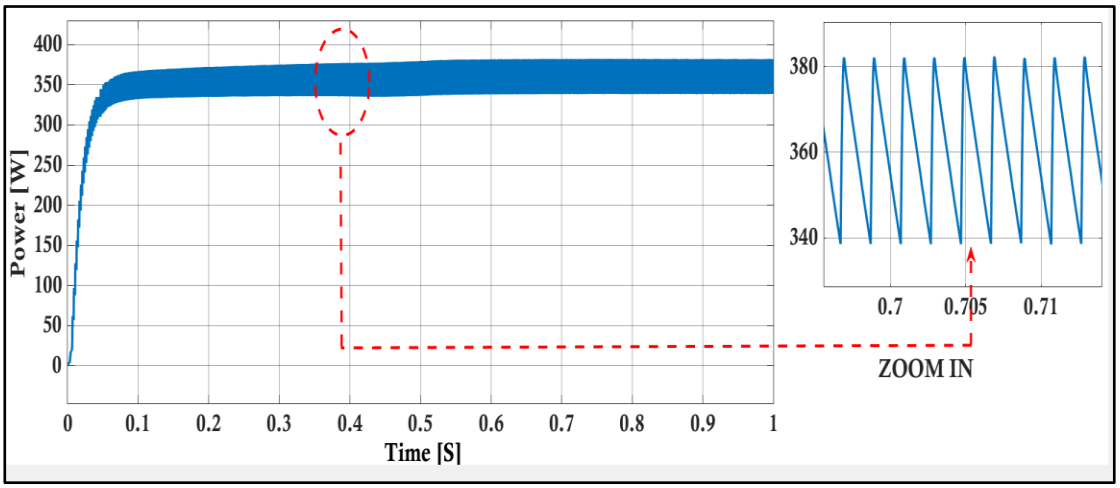

Figure (IV.11): Power Simulation Result

The Figure (IV.11) demonstrates the power stabilization behavior of an MPPT system managed by the Incremental Conductance algorithm.

The primary plot demonstrates a rapid increase followed by stabilization of power at approximately 370W, indicating the system's efficient performance. The zoomed-in view emphasizes periodic fluctuations, illustrating the algorithm's ongoing adjustments to sustain optimal power output. This analysis highlights the ability of the Incremental Conductance algorithm to accurately and dynamically track the maximum power point

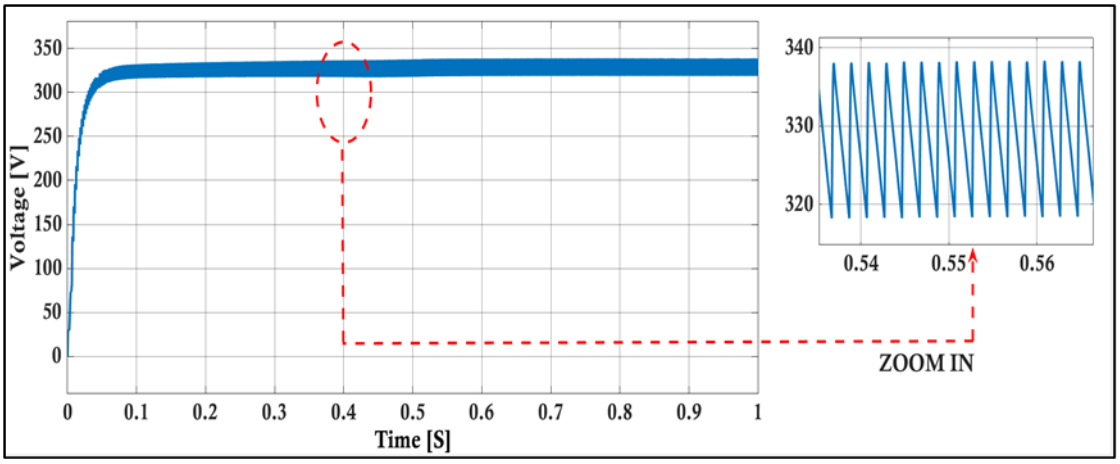

Figure (IV.12): Voltage Simulation Result

Figure (IV.12) illustrates the voltage response of an MPPT system utilizing the Incremental Conductance method.

The primary plot shows the voltage stabilizing at approximately 330V, while the zoomed-in view captures minor fluctuations.

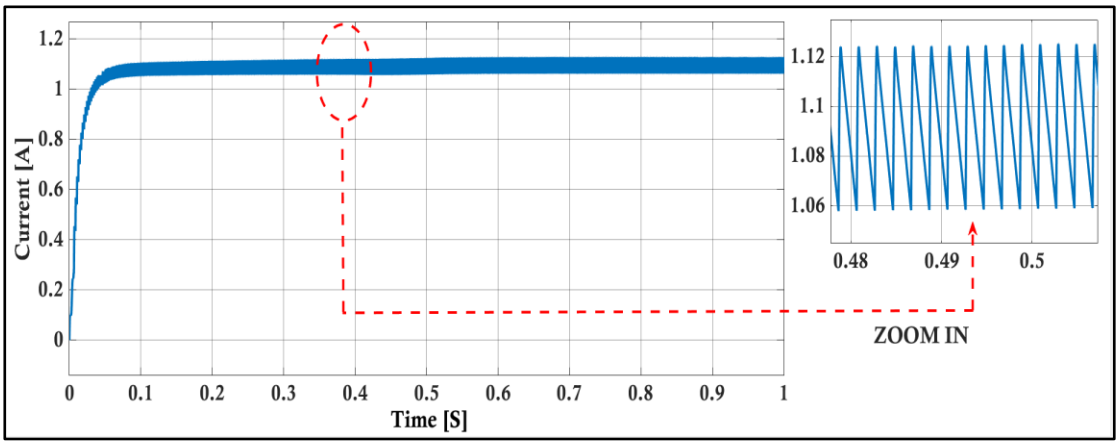

Figure (IV.13): Current Simulation Result

The Figure (IV.13) demonstrates the current stabilization behavior of an MPPT system managed by the Incremental Conductance algorithm.

The main plot demonstrates a rapid increase in current, which stabilizes at approximately 1.1A, reflecting the system's efficiency in reaching the maximum power point. The zoomed-in view accentuates minor fluctuations in the current..

b) Variable Irradiances (1000, 800, 600, 400 W/m^2):

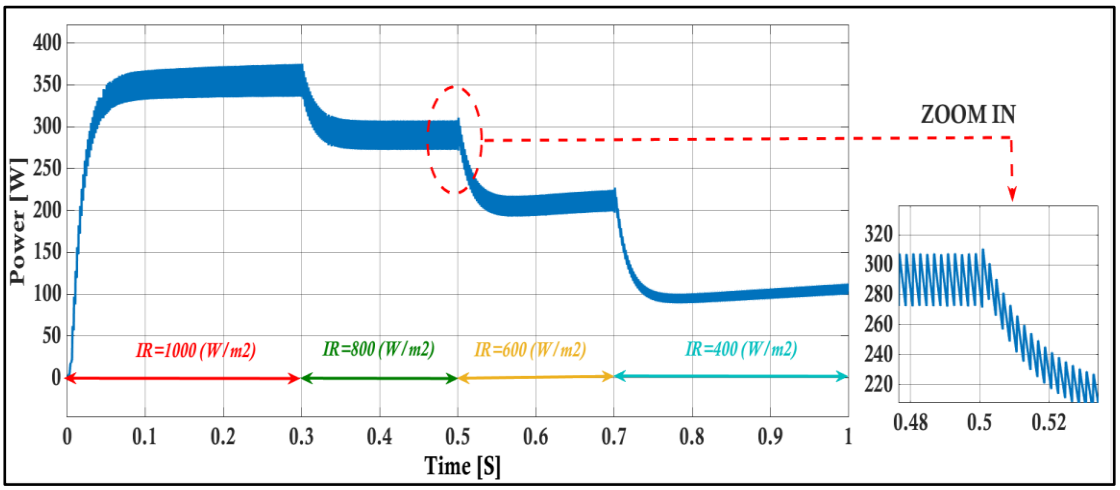

Figure (IV.14): Power Simulation Result

The Figure (IV.14) demonstrates the power response of an MPPT system using the Incremental Conductance algorithm under varying irradiance conditions.

The primary plot illustrates the power stabilizing at approximately 350W initially, followed by stepwise reductions as the irradiance diminishes. The zoomed-in view provides a detailed observation of the transient fluctuations occurring during the change in irradiance.

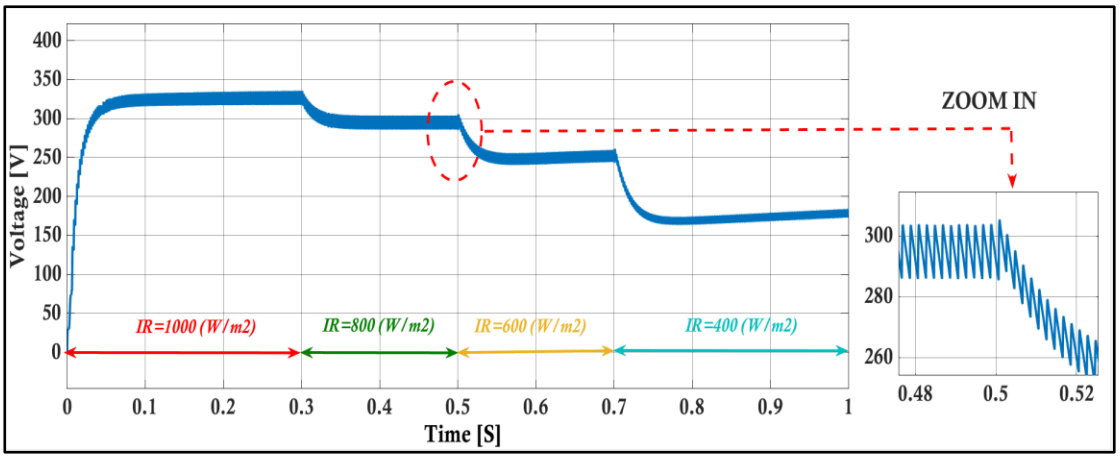

Figure (IV.15): Voltage Simulation Result

The Figure (IV.15) demonstrates the voltage response of an Incremental Conductance-based MPPT system to varying irradiance levels.

The main plot illustrates a rapid increase in voltage, which subsequently stabilizes around 330V, followed by stepwise decreases as the irradiance levels decrease. The zoomed-in view emphasizes the transient fluctuations that occur during these changes

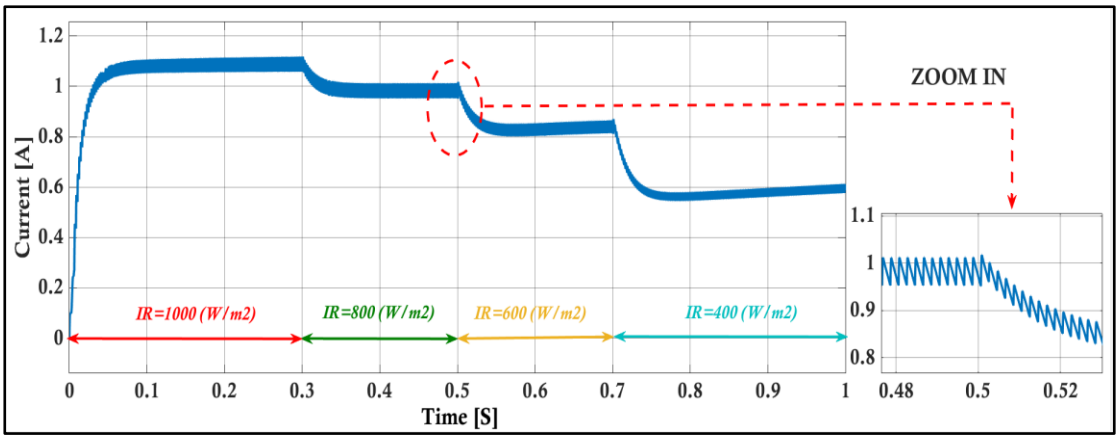

Figure (IV.16): Current Simulation Result

The Figure (IV.16) demonstrates the current response of an MPPT system using the Incremental Conductance algorithm under varying irradiance conditions.

The main plot demonstrates the current stabilizing initially around 1.1A, followed by stepwise reductions as the irradiance decreases. The zoomed-in view

provides a detailed depiction of the transient fluctuations occurring during variations in irradiance..

IV.3.3. Artificial Neural Network (ANN):

In this simulation, we used the Artificial Neural Network (ANN)algorithm to obtain results for power, voltage, and current. Figure (IV.17) represents the general system simulation, showcasing the overall setup and performance of the ANN-based MPPT system. The figure illustrates the integration of PV panels with the ANN-based MPPT controller, which adjusts the duty cycle to optimize power extraction.

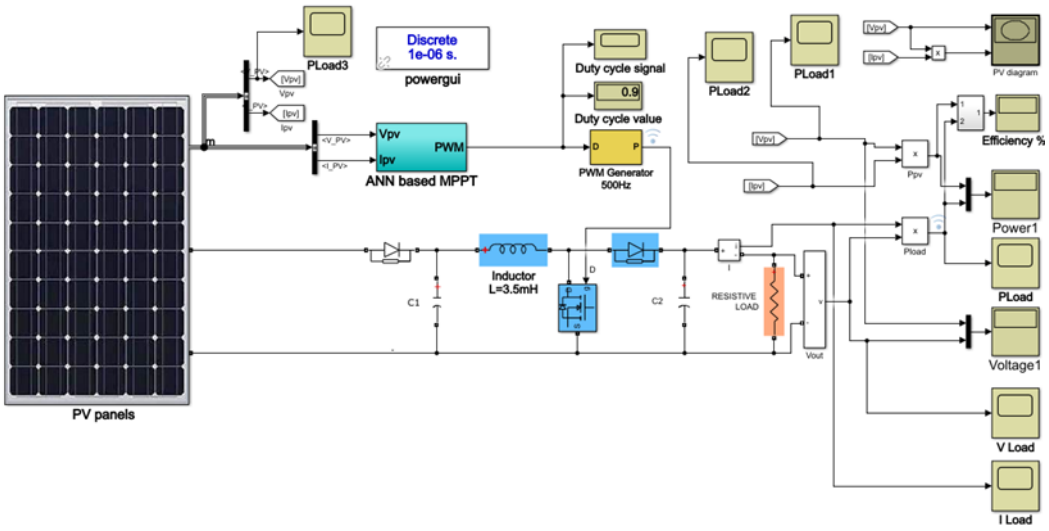

Figure (IV.17): Schema of System Simulation With ANN

a) Constant Irradiance (1000 W/m^2) :

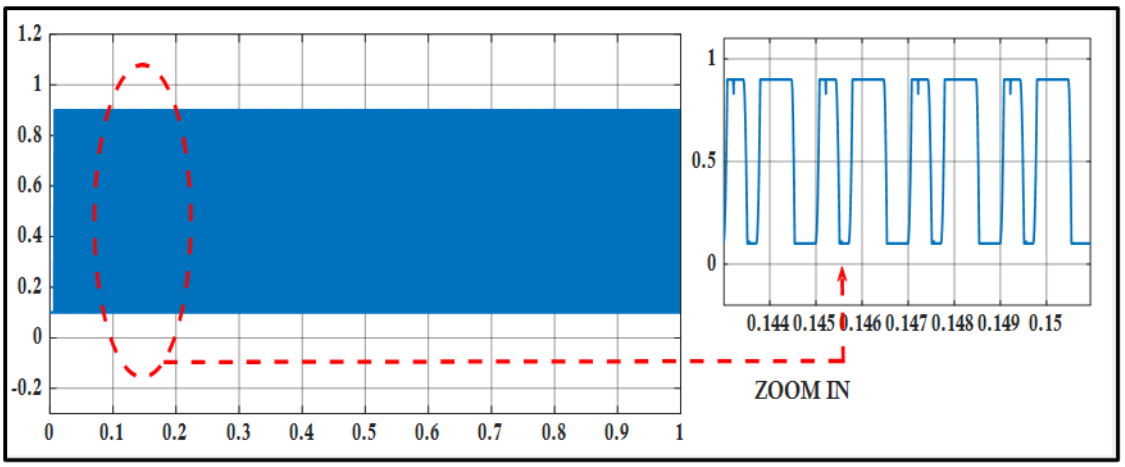

Figure (IV.18): Duty Cycle Simulation Result

The Figure (IV.18) demonstrates the stability and fine-tuning of the duty cycle by an ANN-based MPPT system.

The primary plot illustrates a stable duty cycle close to 1, while the zoomed-in view highlights periodic adjustments, reflecting the artificial neural network's (ANN) responsiveness in optimizing system performance.

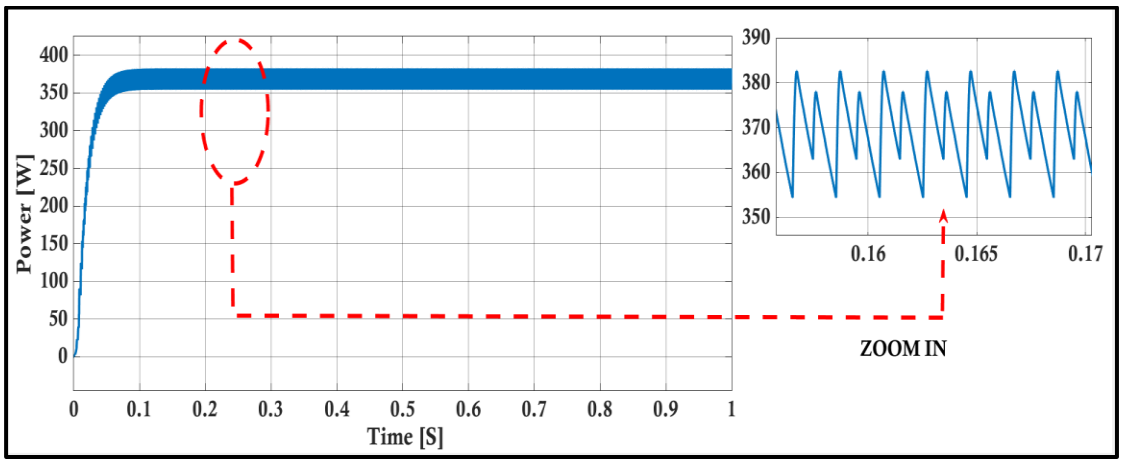

Figure (IV.19): Power Simulation Result

The Figure (IV.19) demonstrates the power stabilization behavior of an MPPT system managed by an ANN algorithm.

The main plot indicates a rapid rise and stabilization of power at approximately 380W, reflecting the system's efficiency. The zoomed-in view highlights periodic fluctuations, illustrating the ANN's ongoing adjustments to maintain optimal power output. This analysis underscores the ANN algorithm's capability to dynamically track the maximum power point with precision.

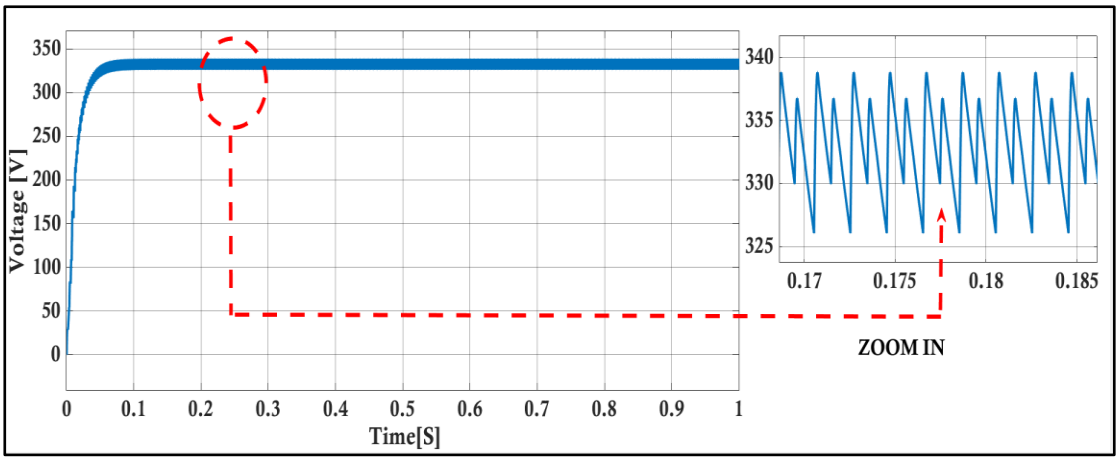

Figure (IV.20): Voltage Simulation Result

The Figure (IV.20) illustrates the voltage behavior of an ANN-based MPPT system. The main plot shows a quick rise and stabilization around 335V, while the zoomed-in view captures small fluctuations.

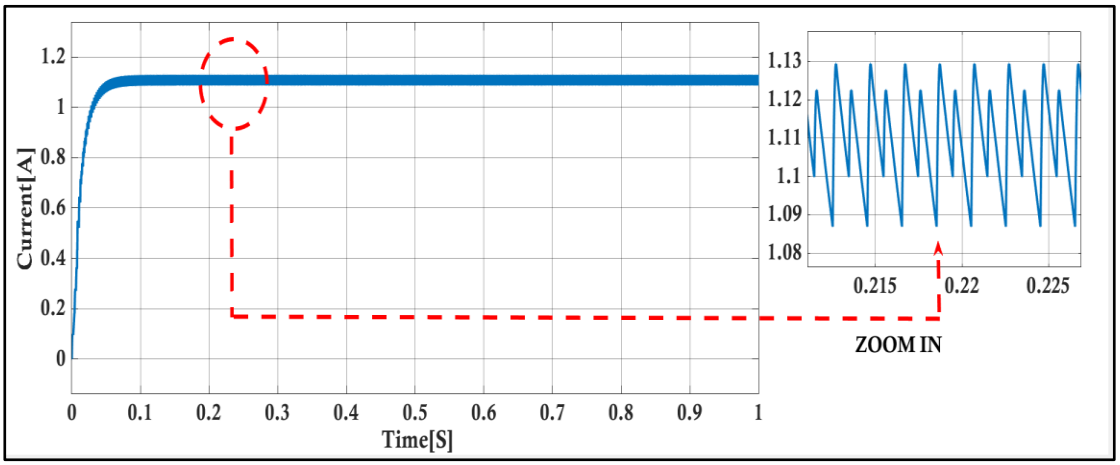

Figure (IV.21): Current Simulation Result

The Figure (IV.21) shows the current stabilization of an ANN-based MPPT system. The main plot displays a rapid rise in current, stabilizing around 1.1A. The zoomed-in view highlights small fluctuations.

b) Variable Irradiances (1000, 800, 600, 400 W/m^2):

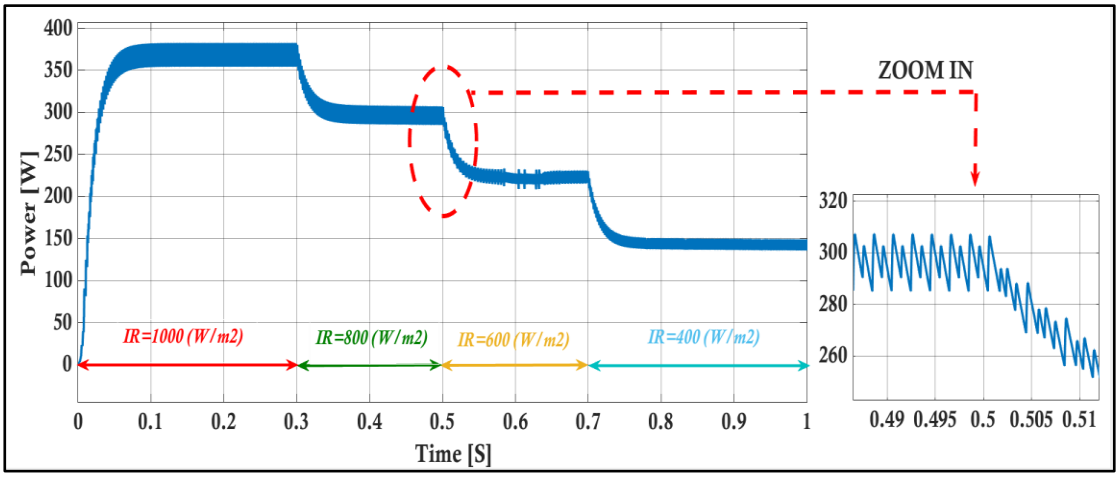

Figure (IV.22): Power Simulation Result

The Figure (IV.22) demonstrates how the ANN-based MPPT system adjusts its power output under varying irradiance conditions.

The primary graph illustrates the stabilization of power at approximately 350W initially, followed by incremental decreases corresponding to reductions in irradiance levels. The enlarged view captures the transient oscillations that occur during variations in irradiance.

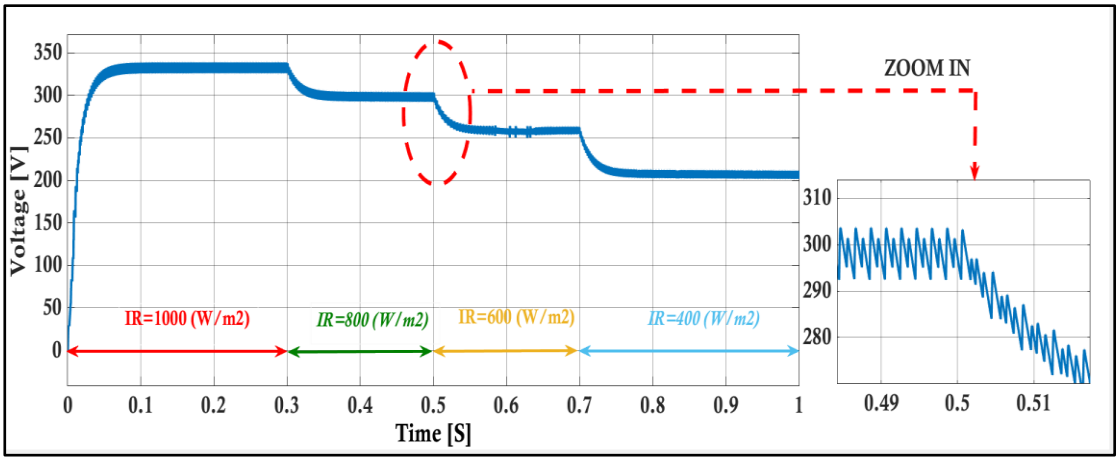

Figure (IV.23): Voltage Simulation Result

The Figure (IV.23) illustrates the ANN-based MPPT system's voltage response to varying irradiance.

The primary graph depicts the voltage stabilizing at approximately 330V, with subsequent reductions corresponding to decreases in irradiance. The zoomed-in view emphasizes transient fluctuations, showcasing the algorithm's ability to dynamically adapt to real-time variations in solar irradiance, thereby ensuring optimal performance.

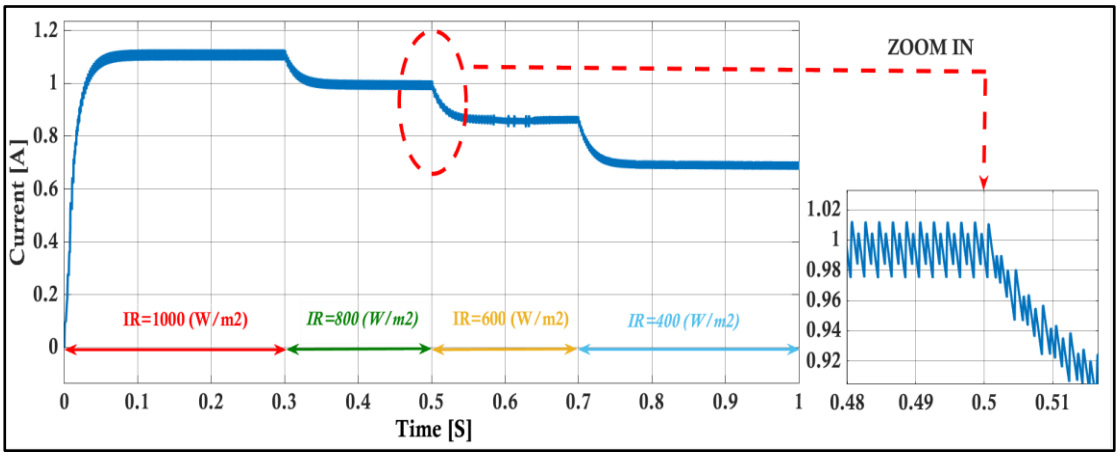

Figure (IV.24): Current Simulation Result

The Figure (IV.24) demonstrates the current response of an ANN-based MPPT system under varying irradiance conditions.

The main plot illustrates the current stabilizing at approximately 1.1A initially, followed by stepwise reductions as irradiance decreases. The zoomed-in view captures the transient fluctuations that occur during changes in irradiance.

IV.4. Comparison and Analysis Between (P&O, INC, ANN):

IV.4.1. Constant Irradiance (1000 W/m^2):

The following figures compare the current and voltage outputs of three MPPT algorithms: Incremental Conductance (INC), Perturb and Observe (P&O), and Artificial Neural Network (ANN).

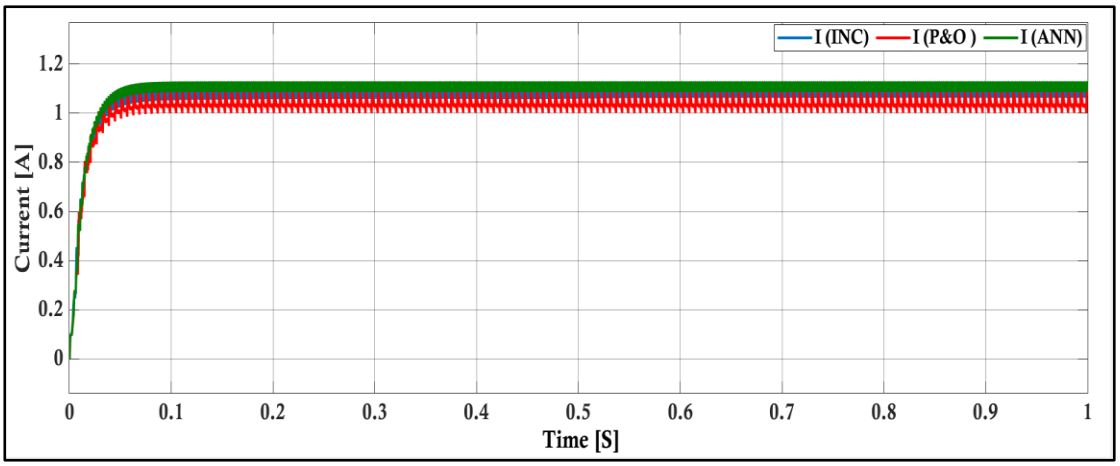

Figure (IV.25): Current Simulation Result

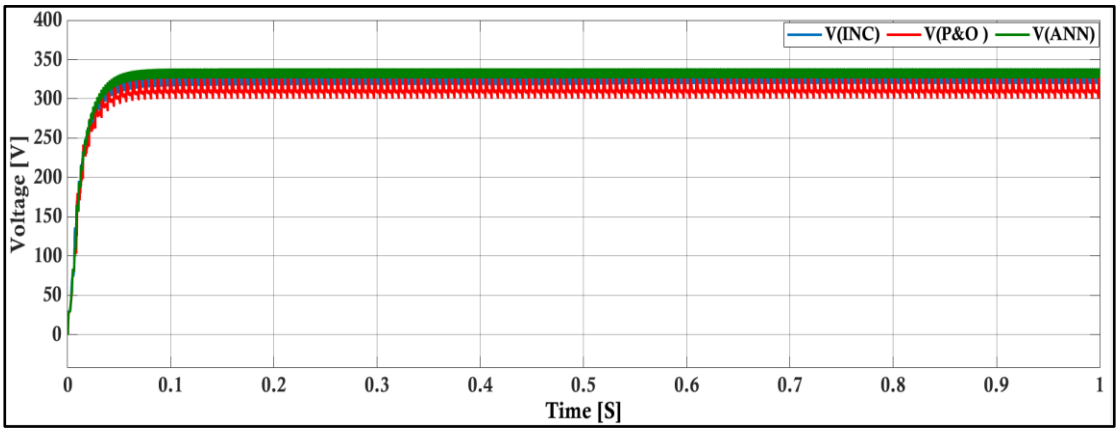

Figure (IV.26): Voltage Simulation Result

IV.4.1.1. Comparison:

- **Incremental Conductance (INC)**: This algorithm shows rapid stabilization in both current and voltage with minimal fluctuations, indicating efficient and stable performance.
- **Perturb and Observe (P&O)**: While it also achieves rapid stabilization, it exhibits more fluctuations in both current and voltage, indicating less stability compared to the other two algorithms.
- **Artificial Neural Network (ANN)**: This algorithm achieves stabilization with minimal fluctuations, similar to INC, suggesting efficient and stable performance.

IV.4.1.2. Analysis:

- **Best Performance**: Both INC and ANN show better performance with minimal fluctuations in current and voltage, suggesting they are more stable and efficient in tracking the maximum power point compared to P&O.
- **Slight Edge**: ANN might have a slight edge over INC due to its adaptive nature and potential for better optimization in varying conditions.

Therefore, based on these figures, the Artificial Neural Network (ANN) algorithm appears to be the best option for MPPT, offering efficient stabilization with minimal fluctuations, closely followed by the Incremental Conductance (INC) algorithm.

IV.4.2. Variable Irradiances (1000, 800, 600, 400W/m^2):

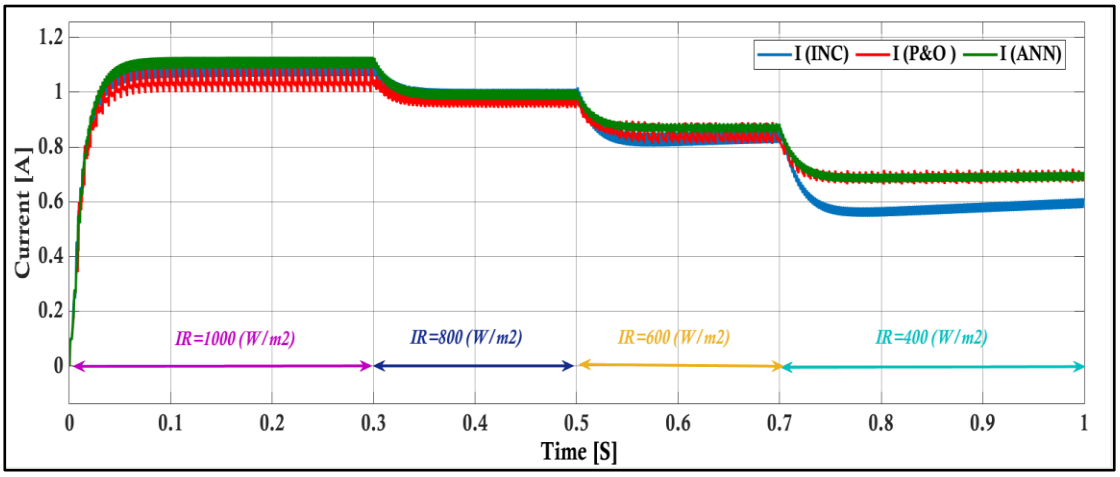

Figure (IV.27): Current Simulation Result

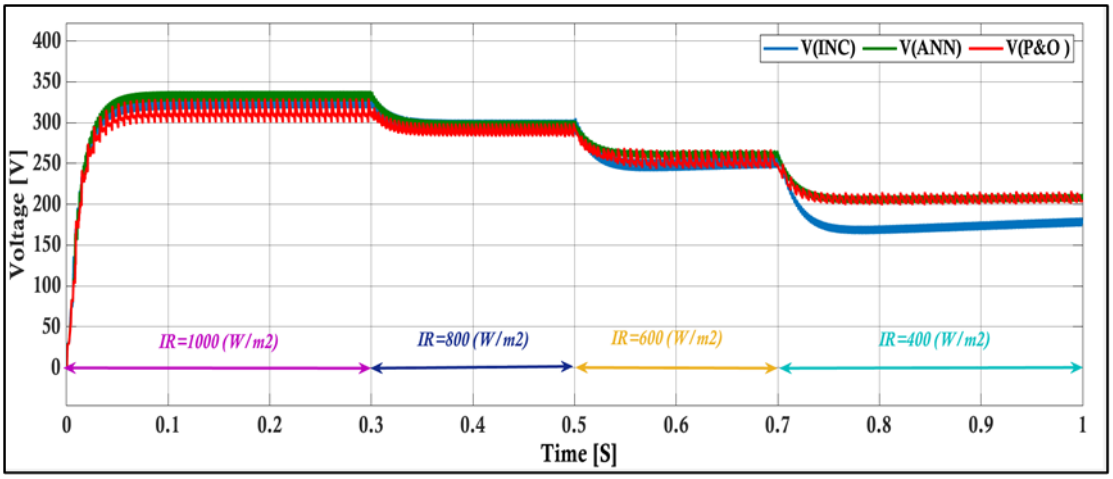

Figure (IV.28): Voltage Simulation Result

IV.4.2.1. Comparison:

- **Incremental Conductance (INC)**: This algorithm shows rapid stabilization but exhibits more fluctuations and deviations during irradiance changes, indicating less stability compared to the other two algorithms.
- **Perturb and Observe (P&O)**: This algorithm shows noticeable fluctuations and is less stable during transitions between irradiance levels.
- **Artificial Neural Network (ANN)**: This algorithm exhibits the least fluctuations and the smoothest transitions during changes in irradiance, indicating the highest stability and efficiency.

IV.4.2.2. Analysis:

- **Best Performance**: The Artificial Neural Network (ANN) algorithm demonstrates the best performance with minimal fluctuations and smooth transitions during varying irradiance levels, indicating superior stability and efficiency.
- **Slight Edge**: The ANN algorithm has a slight edge over the Incremental Conductance (INC) and Perturb and Observe (P&O) algorithms due to its adaptive nature and better optimization in dynamic conditions.

Based on these figures, the Artificial Neural Network (ANN) algorithm appears to be the best option for MPPT, offering the most stable and efficient performance under varying irradiance conditions.

IV.5. Comparison of efficiency between algorithms (P&O, INC, ANN):

IV.5.1. Constant Irradiance (1000 W/m^2):

Algorithm	Efficiency
Perturb and Observe (P&O)	94.72%
Incremental Conductance (INC)	95.58%
Artificial Neural Network (ANN)	96.63%

Table (IV.2): Table of Efficiency

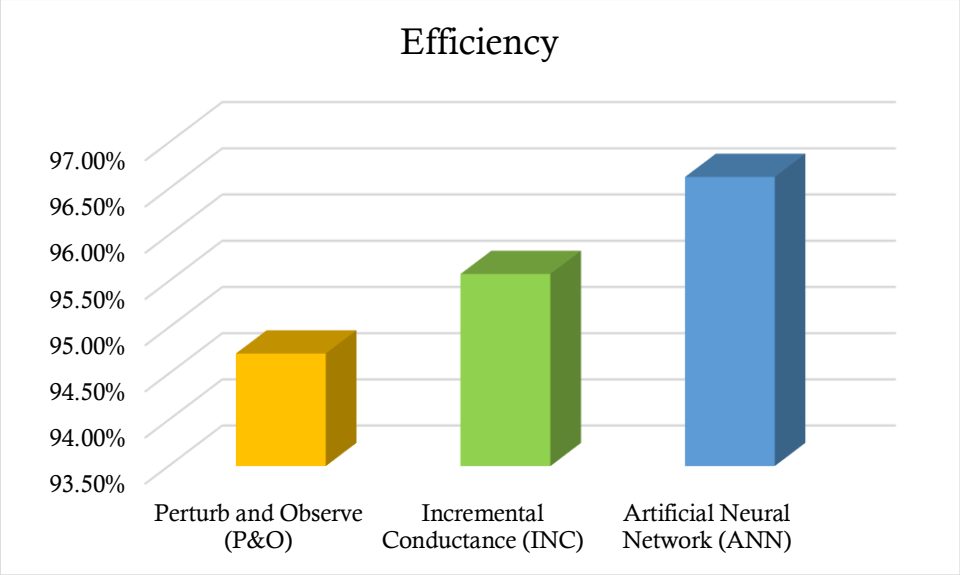

Figure (IV.29): Chart of Efficiency

Under a constant irradiance of 1000 W/m², the Artificial Neural Network (ANN) algorithm exhibits the highest efficiency, approximately 97%. The Incremental Conductance (INC) algorithm achieves an efficiency of around 96%, while the Perturb and Observe (P&O) algorithm demonstrates the lowest efficiency, at approximately 95%. These results suggest that the ANN algorithm is the most effective in optimizing power output under stable irradiance conditions, surpassing both the INC and P&O algorithms in performance.

IV.5.2. Variable Irradiances (1000, 800, 600, 400W/m^2):

Algorithm	Efficiency
Perturb and Observe (P&O)	84.84%
Incremental Conductance (INC)	88.04%
Artificial Neural Network (ANN)	95.06%

Table (IV.3): Table of Efficiency

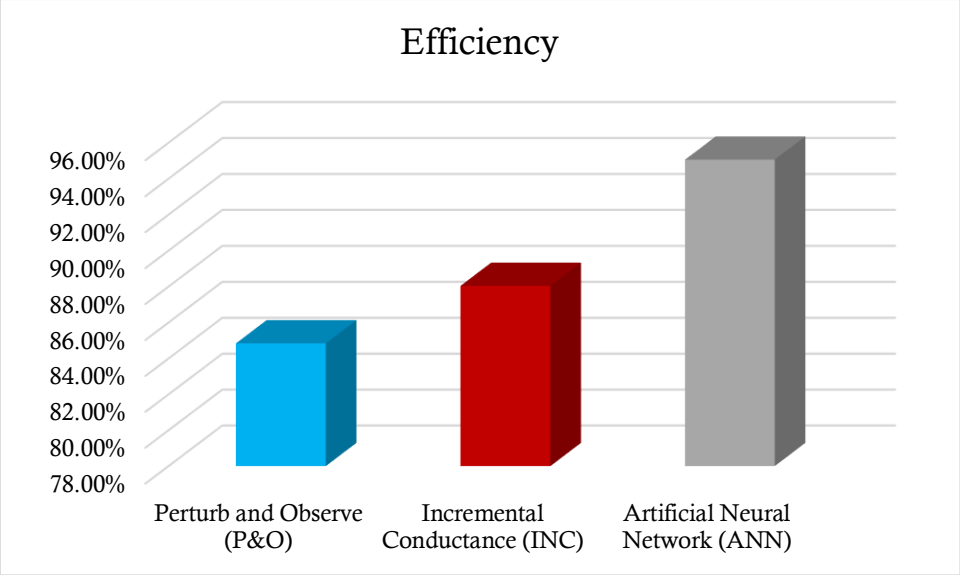

Figure (IV.30): Chart of Efficiency

Under variable irradiance conditions, the Artificial Neural Network (ANN) algorithm achieves the highest efficiency, approximately 95%, demonstrating its superior adaptability to fluctuating light conditions. The Incremental Conductance (INC) algorithm follows with an efficiency of around 89%, indicating reasonable performance but exhibiting less stability in comparison to the ANN algorithm. The Perturb and Observe (P&O) algorithm displays the lowest efficiency, approximately 86%, highlighting its greater vulnerability to variations in irradiance. These findings underscore the ANN algorithm's effectiveness in optimizing power output in dynamic environments.

IV.6. Conclusion:

The Artificial Neural Network (ANN) algorithm stands out as the most effective and reliable MPPT method in this study. Its superior efficiency, stability, and adaptability under both steady and dynamic irradiance conditions make it the best choice for optimizing photovoltaic system output. The Incremental Conductance (INC) algorithm, while performing better than P&O, still falls short of ANN's advanced capabilities. Despite its common use, the Perturb and Observe (P&O) algorithm is the least effective in this comparison, demonstrating lower efficiency and greater instability. Therefore, for maximizing energy extraction and ensuring reliable performance, the ANN algorithm is the recommended MPPT method.

General Conclusion

General Conclusion

This study began by laying the foundation for understanding solar radiation and photovoltaic energy conversion principles. It explained how solar cells harness the photovoltaic effect to generate electricity from sunlight, and discussed the modeling, characteristics, and factors influencing the efficiency of photovoltaic generators. Different photovoltaic cell types based on silicon crystal structures were also presented.

Building upon this, the crucial role of DC-DC converters in power management systems was explored. These converters facilitate efficient voltage conversion through various topologies like buck, boost, and buck-boost, enabling their widespread use across diverse industries.

The concept of Maximum Power Point Tracking (MPPT) was then introduced as a vital technology, particularly for renewable energy systems such as solar power installations. MPPT algorithms optimize energy extraction by continually adjusting the electrical operating point to track the maximum power output of photovoltaic panels.

This naturally led to an in-depth examination of MPPT principles, classifications, and implementation methods. Among the various MPPT algorithms evaluated, the Artificial Neural Network (ANN) approach emerged as the most effective and reliable. Its superior efficiency, stability, and adaptability under both steady and dynamic irradiance conditions make it the recommended method for maximizing energy extraction and ensuring robust performance in photovoltaic systems.

While other algorithms like Incremental Conductance showed better performance than the commonly used Perturb and Observe method, they still fell short of the advanced capabilities offered by ANN-based MPPT. Consequently, for optimizing photovoltaic system output and ensuring long-term, reliable operation, the ANN algorithm stands out as the optimal solution among the methods studied.

References

[1] E. O. Falayi and A. B. Rabiu, solar Radiation Models and Information For. Renewable Energy Applications, Solar Radiation, prof. ElishaB.Babatunde,2012. www.intechopen.com

[2] Julian Chen, translated by Mostafa Mohamed Fouad, reviewed by Mohamed Fathy Khidr, "Solar Energy Physics," Hindawi Foundation, 2011.

[3] Dr. Saud Youssef Ayash, "Alternative Energy Technology," World of Knowledge, Kuwait, February 1981.

[4] Chikha Said, "Optimisation de la puissance dans les systèmes photovoltaïques", RéférenceSusmentionnée, pp 05-07.

[5] Aziz TOULAIT, Rachid Aili, "Modélisation et simulation sous MATALAB/SIMULINK d'unesystèmesphotovoltaïqueapapaptéparunecommandeMPPT", RéférenceSus mentionnée,pp07.

[6] Chika Said, " Optimisation de la puissance dans les systèmes photovoltaïques MEMOIRE DE MAGISTER, Université Larbi Ben M`hidi Oum El Bouaghi Faculté des Sciences et de la Technologie, 2011/2012

[7] BAGHER,A,M. VAHID, M,M,A.MOHSEN,M. Types de cellules solaires et Application. American Journal of Optics and Photonics,2015, 3(5) : 94-113

[8] MEDDOUR Youcef, YAZI Zoubir, "Etude de raccordement d'un système photovoltaïques au réseau réseau électrique ", Mémoire MASTER ACADEMIQUE, UNIVERSITE KASDI MERBAH OUARGLA, Faculté des Sciences Appliquées, 08/06/2015, pp 24.

[9] Aziz TOULAIT, Rachid Aili, "Modélisation et simulation sous MATALAB/SIMULINK d'une système photovoltaïque adaptée par une commande MPPT", Référence Susmentionnée, pp08.

[10] MEDDOUR Youcef, YAZI Zoubir, "Etude de raccordement d'un système photovoltaïques au réseau. réseau électrique", Référence Susmentionnée, pp 24.

[11] Zerouali, Zouirech et al. 2019 [11]

[12] Solar Cell Bag - Arab League Educational, Cultural and Scientific Organization - Tunisia - 2000 AD

[13] Najeeb Saleh Nasr, Ali Misbah Ashtabi, Fawzi Muhammad Aoun, "Laboratory Experiments in the Principles of Photovoltaic and

Electronic Engineering", Dar Al-Kotob Al-Ilmiyah for Publishing, 2002.

[14] Tati Mariam, Bismillah Raja, "The effect of dust on solar photovoltaic panels", Memorandum for the degree of Master of Science in Energy Physics and Renewable Energies Master in Energy Physics and Renewable Energies. Kassidi Merbah University Ouargla. 2019.

[15] Hegedus, S., & Luque, A. (2011). Handbook of Photovoltaic Science and Engineering. John Wiley & Sons

[16] Chauhan, Y. K., & Singh, S. N. (2014). Remote solar-powered applications. IEEE Transactions on Sustainable Energy, 5(1), 132-140.

[17] Abouleija, M. (2011). Design of a photovoltaic water pumping system and its comparison with a diesel pump. Jordanian Journal of Mechanical and Industrial Engineering, 5(3), 273-280

[18] Hanine Mounir and Kebir Allel , "Etude et simulation d'un étage MPPT pour un générateur générateur photovoltaïque à base d'un kit Arduino ", Mémoire de MASTER EN ELECTROTECHNIQUE,UNIVERSITE d'ADRAR,May 25, 2017.

[19]: BENTAYEB MERYEM, "Etude de la commande MPPT à incrémentation de la conductance conductance appliquée aux panneaux solaires", Master's thesis ,Universitaire Belhadj Bouchaib d'Ain-Temouchent,2015 / 2016.

[20] F. L. Luo and H. Ye, Advanced dc/dc converters. crc Press, 2016.

[21] A. S. Y. Alzahrani, Advanced topologies of high-voltage-gain DC-DC boost converters for renewable energy applications. Missouri University of Science and Technology, 2018.

[22] R. P. Severns, G. Bloom, and R. P. Severns, Modern DC-to-DC switchmode power converter circuits. Springer, 1985.

[23] S. Chakraborty, H.-N. Vu, M. M. Hasan, D.-D. Tran, M. E. Baghdadi, and O. Hegazy, "DC-DC converter topologies for electric vehicles, plug-in hybrid electric vehicles and fast charging stations: State of the art and future trends," Energies, vol. 12, no. 8, p. 1569, 2019.

[24] https://www.toolify.ai/ai-news/complete-tutorial-implementing-ann-in-matlabsimulink-1764419#google_vignette (accessed.

[25] M. D. S. M. C. Mr MEKKAOUI Saddam and AhmedYahia, "(Conception, simulation et réalisation d'un régulateur solaire avec

commande MPPT à base d'une carte Arduino) ", UNIVERSITE EchahidHamma Lakhdar- EL Oued, 2022.

[26] M. K. B. Abdelheq, "ETUDE ET REALISATION D'UN CONVERTISSEUR DC-DC," Université Aboubakr BelkaÔd-Tlemcen, 2018.

[27] S. ABBOUDA, "« Contribution à la commande des systèmes photovoltaïques »," Université de Reims Champagne-Ardenne et université de Sfax, 2015.

[28] R. Touahir and M. B. Zahia, "contrôleur neuronal pour la poursuite du point de puissance maximale d'un système photovoltaïque," Mémoire master, Université Kasdi Merbah, Ouargla, Algérie, 2015.

[29] S. H. E. Babaa, "High efficient interleaved boost converter with novel switch adaptive control in photovoltaic application," Newcastle University, 2013.

[30] A. b. T. Bekhti Mohammed, "Maximum Power Point Tracking Simulations for PV Applications Using Matlab Simulink," International Journal of Engineering Practical Research, January 2014.

[31] A. C. Pastor, "Conception et réalisation de modules photovoltaïques électroniques," INSA de Toulouse, 2006.

[32] M. R. Patel, Wind and solar power system. CRC press, 1999.

[33] R. Boukenoui, M. Ghanes, J.-P. Barbot, R. Bradai, A. Mellit, and H. Salhi, "Experimental assessment of Maximum Power Point Tracking methods for photovoltaic systems," Energy, vol. 132, pp. 324-340, 2017.

[34] B. N. Alajmi, K. H. Ahmed, S. J. Finney, and B. W. Williams, "Fuzzy-logic-control approach of a modified hill-climbing method for maximum power point in microgrid standalone photovoltaic system," IEEE transactions on power electronics, vol. 26, no. 4, pp. 1022-1030, 2010.

[35] A. A. Ghassami, S. M. Sadeghzadeh, and A. Soleimani, "A high performance maximum power point tracker for PV systems," International Journal of Electrical Power & Energy Systems, vol. 53, pp. 237-243, 2013.

[36] G. Abdelmounaim, "An Advanced Neural Network-Based MPPT Controller for Photovoltaic Systems," University of El-Oued, 2023.

[37] https://www.toolify.ai/ai-news/complete-tutorial-implementing-ann-in-matlabsimulink-1764419#google_vignette. (accessed.

[38] https://www.mathworks.com/help/deeplearning/ug/workflow-for-neural-network-design.html. (accessed.